IBRO Reports 9 (2020) 164–182

Contents lists available at ScienceDirect

IBRO Reports

journal homepage: www.elsevier.com/locate/ibror

Research Paper

The ameliorative effects of a phenolic derivative of *Moringa oleifera* leave against vanadium-induced neurotoxicity in mice

Olumayowa O. Igado[a,b,c], Anna Andrioli[b], Idris A. Azeez[b,1], Francesco Girolamo[c], Mariella Errede[c], Oluwasanmi O. Aina[a], Jan Glaser[d], Ulrike Holzgrabe[d], Marina Bentivoglio[b], James O. Olopade[a,*]

[a] Department of Veterinary Anatomy, University of Ibadan, Ibadan, Nigeria
[b] Department of Neuroscience, Biomedicine and Movement Sciences, University of Verona, Italy
[c] Department of Basic Medical Sciences, Neurosciences and Sense Organs, University of Bari School of Medicine, Bari, Italy
[d] Institut of Pharmacy and Food Chemistry, University of Würzburg, Germany

ARTICLE INFO

Keywords:
MIMO2
Moringa oleifera
Vanadium
Microglia
Astrocytes
Remyelination

ABSTRACT

Vanadium, a transition series metal released during some industrial activities, induces oxidative stress and lipid peroxidation. Ameliorative effect of a pure compound from the methanolic extract of *Moringa oleifera* leaves, code-named MIMO2, in 14-day old mice administered with vanadium (as sodium metavanadate 3 mg/kg) for 2 weeks was assessed. Results from body weight monitoring, muscular strength, and open field showed slight reduction in body weight and locomotion deficit in vanadium-exposed mice, ameliorated with MIMO2 co-administration. Degeneration of the Purkinje cell layer and neuronal death in the hippocampal CA1 region were observed in vanadium-exposed mice and both appeared significantly reduced with MIMO2 co-administration. Demyelination involving the midline of the corpus callosum, somatosensory and retrosplenial cortices was also reduced with MIMO2. Microglia activation and astrogliosis observed through immunohistochemistry were also alleviated. Immunohistochemistry for myelin, axons and oligodendrocyte lineage cells were also carried out and showed that in vanadium-treated mice brains, oligodendrocyte progenitor cells increased NG2 immunolabelling with hypertrophy and bushy, ramified appearance of their processes. MIMO2 displayed ameliorative and anti-oxidative effects in vanadium-induced neurotoxicity in experimental murine species. This is likely the first time MIMO2 is being used *in vivo* in an animal model.

1. Introduction

Heavy metals persist for a very long time in the environment and so severely affect human health through the food chain (Verma and Dubey, 2003). Vanadium (V) is a heavy metal with a wide distribution in the world (World Health Organization (WHO, 2001). Vanadium is a metal of the transition series, with atomic number 23. It is used extensively in the chemical industry (Cui et al., 2015) and is released into the atmosphere during fossil fuel burning (Osuji and Avwiri, 2005), through forest fires, volcanic emissions and marine aerosols (Englert, 2004). Vanadium crosses the blood brain barrier (Olopade and Connor, 2010) and its administration in experimental animals have been reported to result in demyelination, microglia and astrocyte activation, tumour necrosis factor and interleukin 1β expression, and locomotion and cognition deficits (García et al., 2004, 2005; Igado et al., 2012; Mustapha et al., 2014; Azeez et al., 2016).

Different compounds have been postulated to treat the neurotoxic effects of vanadium *in vivo*, for example vitamin E (Olopade et al., 2011), *Garcinia kola* seeds and kolaviron (Igado et al., 2012) and erythropoietin (Mustapha et al., 2014); but each of these compounds have displayed limitations, in that erythropoietin use may be limited due to its cost, and *Garcinia kola* seeds showed severe pro-oxidative effects at the dose used to treat vanadium neurotoxicity.

Moringa oleifera is a multipurpose plant, belonging to the family *Moringaceae*, and widely distributed throughout Africa and Asia (Iqbal and Bhanger, 2006). The leaves are reputedly rich sources of potassium, calcium, phosphorus, iron, vitamins A, C and D, essential amino acids and antioxidants (vitamin C, β-carotene, flavonoids) (Bamishaiye et al., 2011), and other compounds like alkaloids, tannins, phenolics, saponins and steroids (Sutalangka et al., 2013). Due to the high presence of

* Corresponding author at: Department of Veterinary Anatomy, University of Ibadan, Nigeria.
E-mail address: jo.olopade@mail.ui.edu.ng (J.O. Olopade).
[1] Present Address: Department of Veterinary Anatomy, University of Jos, Jos, Nigeria.

https://doi.org/10.1016/j.ibror.2020.07.004
Received 12 March 2020; Accepted 3 July 2020

phenolic compounds in the leaves, it is believed to have a good antioxidative activity (Igado et al., 2018), and this is why the leaves and derivative compounds from it have been used by different authors to treat different forms of neurodegenerative diseases and neurotoxicity, *in vitro* and *in vivo* (Bakre et al., 2013; Hannan et al., 2014; Galuppo et al., 2014; Giacoppo et al., 2015; Igado et al., 2018).

Our study demonstrates the neuroprotective potential of MIMO2 (which was obtained from the methanolic extract of *M. oleifera* leave as previously described in an earlier experiment by us (Igado et al., 2018) in vanadium-induced neurotoxicity in young mice.

2. Materials and methods

2.1. Animals and treatment

MIMO2 was obtained as previously described by Igado et al. (2018). Ethical approval was obtained from the Animal Care and Use Research Ethics Committee (ACUREC) of the University of Ibadan, ethical code number UI-ACUREC/App/2016/028. All experiments and handling of the mice were in accordance with the National Institute of Health Guide for the Care and Use of Laboratory Animals (NIH Publications No. 80-23), revised 1996. The guidelines for toxicity studies by the Organization for Economic Cooperation and Development (OECD), Section 4, Numbers 417, 424 and 426 were taken into consideration in establishing the LD_{50} of MIMO2 and also when administering it in combination with vanadium. To calculate the LD_{50} of MIMO2 and the dose to be used with vanadium, two major experiments were performed, first, with MIMO2 alone and secondly, MIMO2 at different doses in combination with vanadium 3 mg/kg.

2.1.1. Calculating the median lethal dose (LD_{50}) of MIMO2

MIMO2 being insoluble in water was diluted with sterile dimethyl sulphoxide (DMSO) and was administered intraperitoneally (i/p) in all cases. Duration of dosing was based on a modification of the methods by Lindamood et al. (1992) and Stewart et al. (2008) and based on the fact that reports of neuropathologies from vanadium administration were observed from treatment for 5 consecutive days and above (García et al., 2004, 2005; Igado et al., 2012). Four-week old male albino mice were used to ascertain the median lethal dose (LD_{50}) of MIMO2 based on a modification of Lorke's method (1983). Sixteen 4-week old male mice were assigned randomly into 4 groups and administered 100 mg/kg, 75 mg/kg, 50 mg/kg and 25 mg/kg of MIMO2 on a daily dose for eight days. Mortality was recorded.

Results obtained were used to calculate the LD_{50} based on Lorke's formula:

$$LD50 = \sqrt{(D0\,x\,D100)}$$

Where D0 = highest dose that gave no mortality (25 mg/kg), and D100 = lowest dose that produced mortality (50 mg/kg).

$$LD50 = \sqrt{(25\,x\,50)} = 35.35 \text{ mg} \approx 35 \text{ mg/kg}$$

2.1.2. Arriving at the Optimal MIMO2 Dose used in combination with vanadium 3 mg/kg

A pilot study was initially conducted to assess the effect of MIMO2 and vanadium on mortality and morbidity. Sixteen 4-week old male mice were randomly divided into 4 groups of 4 mice each, receiving the dose of 35 mg/kg, 25 mg/kg, 15 mg/kg and 10 mg/kg.

Vanadium, administered as sodium metavanadate 3 mg/kg (hereafter referred to as vanadium 3 mg/kg) was adopted as the demyelinating but none-lethal dose according to García et al. (2004, 2005). This dose has been confirmed by other authors (Igado et al., 2012; Azeez et al., 2016; Mustapha et al., 2014).

Combining vanadium 3 mg/kg with MIMO2 35 mg/kg for 8 days resulted in mortality of the mice. Vanadium and MIMO2 were administered i/p, for 8 consecutive days. Vanadium was dissolved in sterile water.

2.1.3. Effect of MIMO2 on vanadium induced neurotoxicity in developing mice

Eighty-four 2-week old mice (both male and female) were randomly divided into seven groups of 12 mice each. Both sexes were used since sexual maturity is not attained until 6 weeks (Drickamer, 1981)

Group I – Negative control (sterile water – H_2O)
Group II – Vanadium 3 mg/kg (V)
Group III –Vanadium 3 mg/kg + MIMO2 10 mg/kg (V + M10)
Group IV – MIMO2 10 mg/kg (M10)
Group V –Vanadium 3 mg/kg + MIMO2 5 mg/kg (V + M5)
Group VI – MIMO2 5 mg/kg (M5)
Group VII – Negative control II (DMSO)

DMSO was added as an experimental group to ascertain that there were no pathologies associated with its administration.

Treatment was for 14 days. All injections were administered i/p. Vanadium was administered daily, while MIMO2 was administered at day 0, after 48 h (h) and every 72 h thereafter(D0, D2, D5, D8, D11, D14). Mice were subjected to neurobehavioural tests on D14 and sacrifice of 5 mice per group was done on D15 (Charan and Kantharia, 2013).

2.1.4. Neurobehavioural tests

Two neurobehavioural tests were carried out to test for muscular strength and coordination (hanging wire test) and to test for anxiety (open field test). Twelve mice were sampled for each group as required for neurobehavioural tests (Olopade et al., 2012). The protocol for the neurobehavioural tests was adapted from Mustapha et al. (2014) and Azeez et al. (2016).

Hanging wire test: Mice were suspended by their forelimbs from a wire, at a height of about 60 cm from the ground. The time it took for each mouse to fall off the wire was recorded in seconds. A trial of 3 times was conducted for each mouse and the average time calculated.

Open field test: A white open wooden box, measuring 80 cm by 80 cm, with 16 smaller squares (demarcated with black paint) measuring 20 cm by 20 cm, and a centre square measuring 20 cm by 20 cm. The mouse was placed in the centre square and released. The duration of the stay in the box was 5 min per animal. The number of line crossings, rearing, grooming, number of faecal boluses voided, and urine spots were noted. The average values for these parameters were calculated per group. ANY-maze® software (Stoelting Co, IL, USA), version 4.99 m, was used to analyse the open field test.

2.1.5. Body and relative brain weight

Body weight was recorded daily for all the groups using a digital weighing scale (Camry®, China). Daily weight increase was achieved by comparing increase in body weight relative to postnatal day14, which was the start of the experiment (D1). Calculation was Dx – D1, where 'x' is the particular day of concern after the commencement of the experiment.

For ethical reasons, five mice were sacrificed per group. After sacrifice, the brains were harvested and weighed immediately. Relative brain weight was calculated in each animal as $\left(\frac{Brain\ Weight}{Body\ weight}\right)x\,100$, and expressed in percentage.

2.1.6. Sacrifice of mice

Five mice per group (Charan and Kantharia, 2013) were sacrificed on D15. All mice were anaesthetized with ketamine (100 mg/kg, i.p.). Mice were perfused transcardially with 4 % paraformaldehyde (PFA) in 0.1 M phosphate buffer, pH 7.4. The brains were post-fixed in PFA for 2 h and stored in 0.1 % Na (Sodium) azide in 0.1 M phosphate buffered saline (PBS) at 4 °C until ready for sectioning. Brains were then placed in 30 % sucrose in PBS for cryoprotection for 24 h. Serial coronal sections were cut through the brain at a 30 μm thickness with a freezing

microtome, collected in adjacent wells of 24-well plates and kept at 4 °C until analysed.

2.1.7. Histopathology

Haematoxylin and Eosin (H and E) stain: Histopathological features in brain regions (cerebral cortex and subcortical white matter, cerebellum and the hippocampus) were assessed. Brain sections mounted on slides were immersed in haematoxylin for about 30 s, rinsed in tap water until water was clear, slides were transferred to eosin stain for about 1 min, rinsed again and thereafter dehydrated in ascending concentrations of alcohol (50 %, 70 %, 80 %, 95 %, and 100 %). Sections were cleared in xylene and cover-slipped with Entellan (Merck, Darmstadt, Germany).

Cresyl violet stain: This stain was used to count hippocampal cells in the CA1 and CA3 regions. The cell count of total percentage of dead cells was calculated as $\left(\frac{Number\ of\ dead\ cells}{Total\ number\ of\ cells}\right)x100$. The dead cells were differentiated from the healthy cells by their vacuolated and pyknotic appearance. Brain sections were mounted on slides and immersed in chloroform/ethanol solution (4:1) for 1 h, and thereafter placed in cresyl violet solution (Sigma-Aldrich, Germany) for about 10 min. The sections were then dehydrated in ascending concentrations of ethanol, cleared in xylene and cover-slipped with Entellan (Merck, Darmstadt, Germany).

2.1.7.1. Black gold II myelin histochemistry. Series of adjacent brain sections from all groups were processed in parallel for myelin staining using the Black Gold II (BGII) histochemical protocol according to a modification of the method previously described by Schmued et al. (2008) and published by Azeez et al. (2016). Briefly, the sections were washed in distilled water for 2 min before adding a 0.3 % warm Black-Gold (haloaurophosphate complex) (HistoChem, Jefferson, AR, USA) solution, obtained by adding 100 mg of Black- Gold to 50 mL of 0.9 % NaCl and then heating to 60 °C. The sections were then incubated in an oven for 18 min at 60 °C. The staining was monitored visually for 12 − 18 min until full impregnation. The sections were mounted on gelatin coated slides, air-dried for 24 h, and then dehydrated through graded alcohols, cleared in xylene and cover slipped with Entellan (Merck, Darmstadt, Germany) as mounting medium. BGII counterstained with cresyl violet stain was also employed to assess the brain histology.

2.1.7.2. Immunohistochemistry: myelinated axons, astrocytes and microglia. Brain sections were processed for immunoperoxidase method to investigate microglia and astrocyte activation, and the eventual occurrence of damage of myelinated axons, assessed by the presence of nonphosphorylated neurofilaments, a sensitive marker of axonal pathology. Sections were first treated in 0.1 % H_2O_2 (Mallinckrodt Baker, Deventer, The Netherlands) for 15 min to inactivate endogenous peroxidase and then incubated for 1 h in 5 % normal goat or horse serum (Vector Labs, Burlingame, CA, USA) in PBS. The sections were then incubated overnight at 4 °C in PBS containing 1 % normal goat or horse serum and the following primary antibodies: rabbit anti-glial fibrillary acidic protein (GFAP) (1: 500; Merck, Darmstadt, Germany), to visualize astrocytes; rabbit monoclonal anti-Iba-1 (1:1500; Wako, Japan) for visualising microglia. After washing, the sections were incubated for 2 h at room temperature (RT) in the appropriate biotinylated secondary antibodies (diluted 1:200; all purchased from Vector Labs). The sections were then reacted in avidin biotin solution (ABC kit, Vectastain, Vector Labs) and finally visualized using 3,3′-diaminobenzidine as chromogen and peroxide. Sections were then dehydrated in graded alcohols, cleared in xylene, mounted on gelatinized slides, and cover slipped with Entellan.

The brain sections were also processed for immunofluorescence to reveal astrocytes. These sections were first rinsed in PBS, incubated for 1 h at RT with a blocking solution containing normal donkey serum, and then incubated overnight at RT, on a rocker with primary antibody rabbit anti-GFAP (1:500, DAKO, Glostrup, Denmark). Anti-rabbit IgG Alexa 647 (Invitrogen, Thermo Fisher Scientific, Waltham, MA, USA) was used as secondary antibody. The sections were then counterstained with the fluorescent nuclear marker 4′-6′-diamidino-2-phenylindole diluted (DAPI (Santa Cruz Biotechnology, Santa Cruz, CA, USA) 1:100.000 in PBS for 10 min, mounted on slides with 0.1 % para-phenylendiamine in a glycerol-based medium (90 % glycerol and 10 %

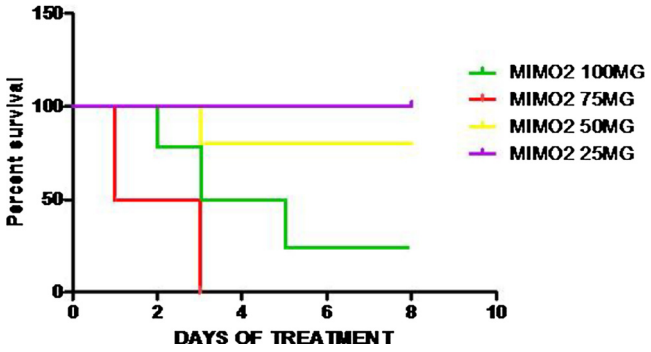

Fig. 1. LD_{50} of MIMO2. Kaplan-Meier survival graph, an 8-day experiment showing the mortalities and the days recorded in 4- week old mice. MIMO2 100 mg - D2 ($^1/_4$), D3 ($^2/_4$), D5 ($^3/_4$); MIMO2 75 mg/kg – D1 ($^2/_4$), D3 ($^4/_4$); MIMO2 50 mg/kg – D3 ($^1/_4$), MIMO2 25 mg/kg – No mortality recorded. Number of mice per group = 4.

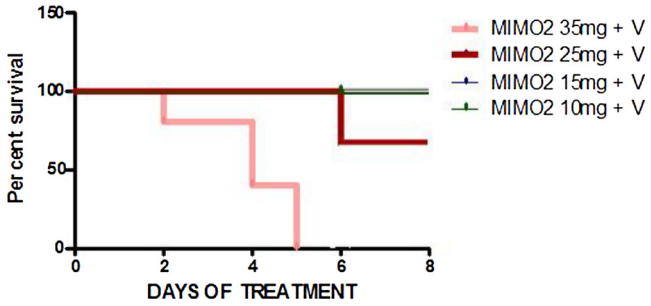

Fig. 2. MIMO2 + Vanadium 3 mg/kg (V). Kaplan-Meier survival graph, an 8-day experiment showing the mortalities and the days recorded in 4-week old mice. MIMO2 35 mg/kg + V– D2 ($^1/_5$), D4 ($^3/_5$), D5 ($^5/_5$); MIMO2 25 mg/kg + V– D6 ($^3/_4$); MIMO2 15 mg/kg + V and MIMO2 10 mg/kg + V– No mortality recorded (100 % survival). Note: values for MIMO2 15 mg/kg + V and MIMO2 10 mg/kg + V are similar resulting in superimposition of lines in graph. Number of mice per group = 4 or 5..

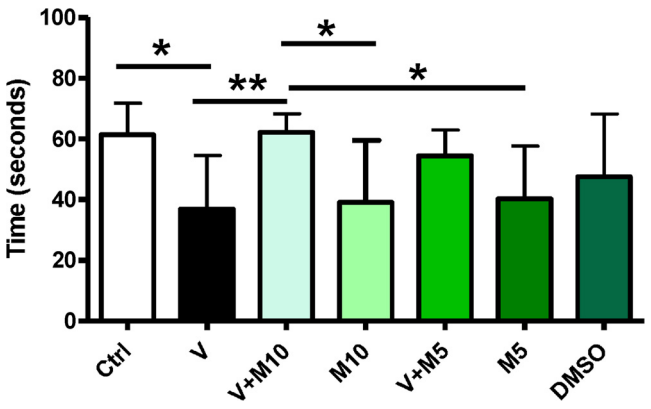

Fig. 3. Neurobehavioural Test – Hanging wire. Highest values recorded in the control group and M10 + V 3 mg/kg. Groups – Ctrl (sterile H_2O – control); V (Vanadium 3 mg/kg); V + M10 (Vanadium 3 mg/kg + MIMO2 10 mg/kg); MIMO2 10 mg/kg; MIMO2 5 mg/kg; V + M5 (Vanadium 3 mg/kg + MIMO2 5 mg/kg); DMSO: dimethyl sulphoxide. Number of mice per group = 12. (*p < 0.05, **p < 0.01).

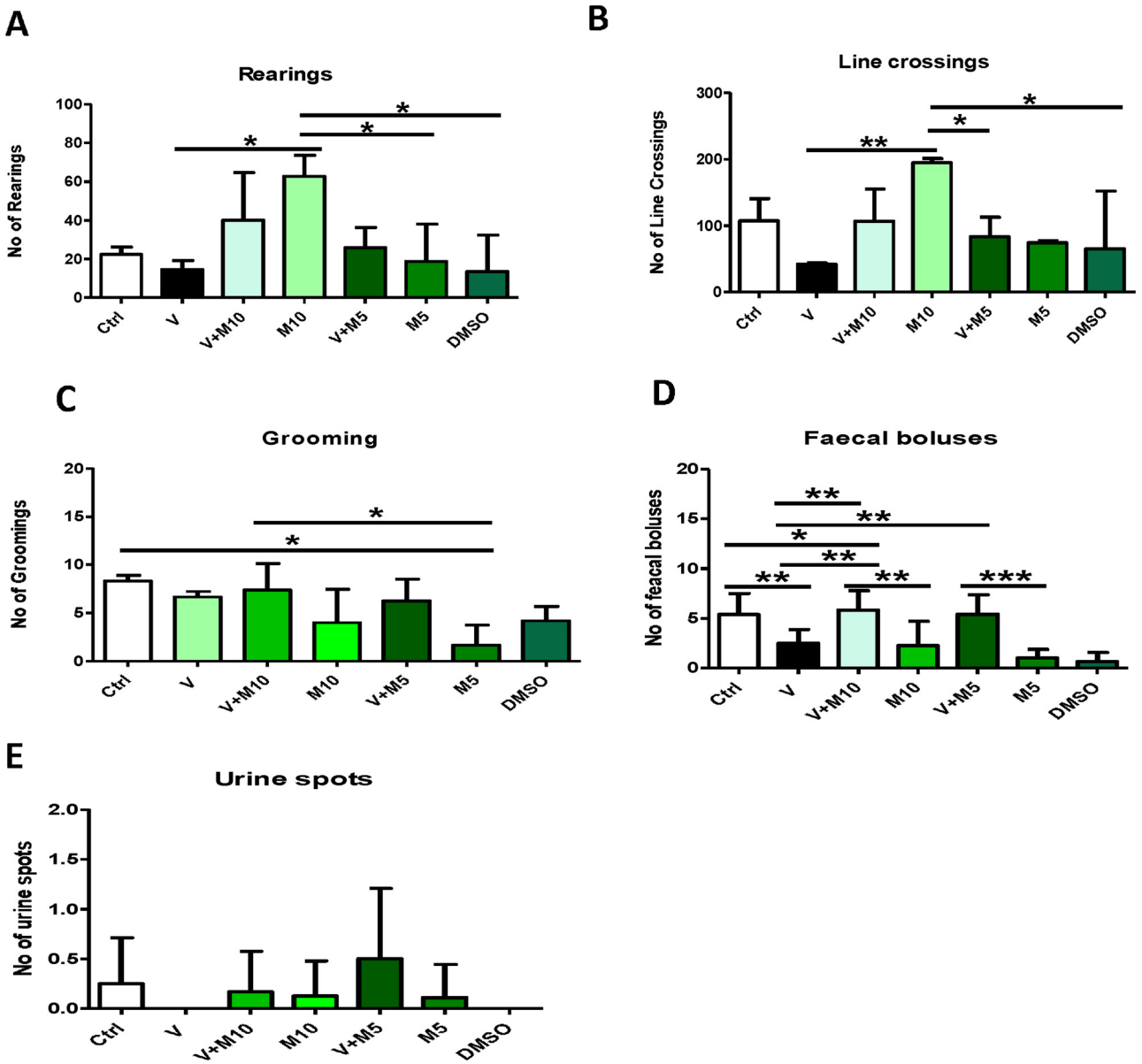

Fig. 4. Open Field Test. Groups – Ctrl (sterile water); V (Vanadium 3 mg/kg); V + M10 (Vanadium 3 mg/kg + MIMO2 10 mg/kg); M10 (MIMO2 10 mg/kg); M5 (MIMO2 5 mg/kg); V + M5 (Vanadium 3 mg/kg + MIMO2 5 mg/kg); DMSO: dimethyl sulphoxide. Number of mice per group = 12. (*p < 0.05, **p < 0.01, ***p < 0.001).

PBS) and cover-slipped.

2.1.7.3. Immunohistochemistry: oligodendrocyte lineage cells, myelin and axons. Following Black-Gold II histochemistry for initial screening of myelination, immunohistochemistry for myelin, axons and oligodendrocyte lineage cells were then investigated according to the protocols described by Girolamo et al. (2011). The following primary antibodies were utilized in single and double immunofluorescence: rabbit anti-myelin basic protein (MBP; 1:100; Abcam ab65988, Cambridge, UK), rabbit anti-nerve-glial antigen 2 (NG2; 1:180; Millipore AB5320, Merck, Darmstadt, Germany), rabbit anti-glutathione S-transferase isoform-π (GST; 1:700, MBL Int. Corp. Cat. 312, Woburn, MA, USA), mouse anti- 200 kDa neurofilament (NF; 1:1000, BioLegend, SMI31R, San Diego, CA, USA). Briefly, after permeabilization (0.5 % Triton X-100 in PBS), free-floating sections were incubated with single or combined primary antibodies overnight at 4 °C, detected by appropriate fluorophore-conjugated secondary antibodies for 45 min at RT and then counterstained with TO-PRO-3 (Alexa Fluor® 633, diluted 1:10,000 in PBS; Invitrogen). Finally, the sections were collected on Vectabond™ treated slides (Vector) and cover-slipped with Vectashield (Vector). Negative controls were prepared by omitting the primary antibodies or mismatching the secondary antibodies.

2.2. Microscopy and quantitative analyses

CA1 and CA3 cell count: After staining sections with cresyl violet, photomicrographs of the CA1 and CA3 regions of the hippocampus were obtained at x400 magnification. Using Motic Images Plus 2.0 software (Hong Kong, Asia), rectangular boxes were generated to capture and determine the area of cell count at specific regions. The density of the cells in a determined area was calculated as result of total cell count in the rectangular boxes divided by total area of the boxes generated.

Densitometric analysis: This was employed to analyse the Black Gold intensity of the commissural region of the corpus callosum, using the

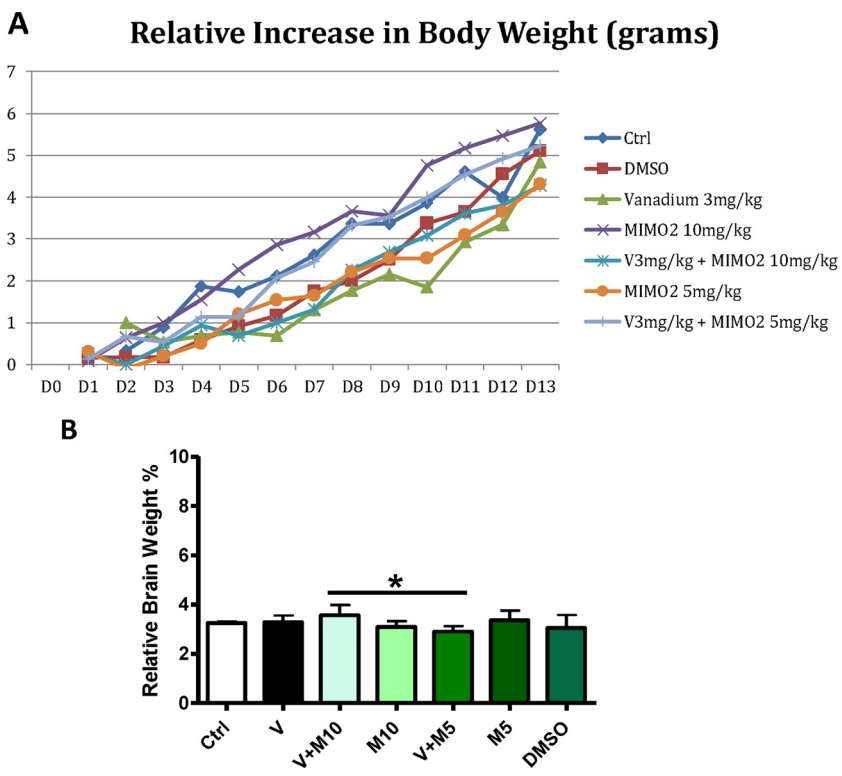

Fig. 5. A is the line graph showing the relative increase in body weight in grams (D1 – D13) of the different experimental groups. B shows the mean relative brain weights of the groups, expressed as percentage. No statistically significant difference ($p > 0.05$) was observed among the groups when compared with the control group (H_2O) and V3 mg/kg group. Groups – Ctrl (H_2O – control); V (Vanadium 3 mg/kg); V + M10 (MIMO2 10 mg/kg + Vanadium 3 mg/kg); M10 (MIMO2 10 mg/kg); V + M5 (MIMO2 5 mg/kg + Vanadium 3 mg/kg); M5(MIMO2 5 mg/kg); DMSO: dimethyl sulphoxide. Number of mice per group = 12. (*$p < 0.05$).

Olympus microscope Image Pro Plus® software (http://www.neurosciencecourses.com/uploads/3/4/4/9/34494139/sns_poster_pdf.pdf). Stereological microglial cell count was conducted with the Stereo-investigator software (Micro Bright Field Europe, Magdeburg, Germany), while the microglia percentage area covered was assessed with the Image Pro Plus® software (Media Cybernetics, Rockville, MD, USA) (Azeez et al., 2016; Palomba et al., 2015).

The sections stained with BGII were observed under bright-field illumination, and pictures were acquired with QUICAM Fast 1394 camera connected to the Olympus BX51 microscope. The sections processed for immunofluorescence were examined under a Leica TCS SP5 confocal laser scanning microscope (Leica Microsystems, Mannheim, Germany) using a sequential scan procedure. Confocal images were taken at 0.45 µm intervals through the z-, x-, and y-axes of the section with 40x and 63x oil lenses and used for quantitative analyses according to Girolamo et al. (2011). All observations and analyses were performed blindly of the experimental group assignment.

Astrocytes and microglia were qualitatively assessed for activation and non-activation state, based on the appearance of the cell bodies and processes, and also increase in percentage of the total area covered by Iba-1$^+$ microglia.

The quantitative analysis of the Iba-1$^+$ microglia (percentage area covered) was analysed based on the method of Azeez et al. (2016). Images were obtained using a QUICAMFast 1394 camera connected to an Olympus BX51 microscope. Images were obtained at x20 objective. A standardised stereological method was employed to analyse immune-stained sections using Image Pro Plus 7.0 Software. Five equidistantly positioned frames were incorporated into the area of interest. Iba-1$^+$ microglia immunopositivity for the cell body and processes was measured in each frame and converted automatically by the software in estimated surface, taking into account the thickness of the sample. The background intensity was calculated and served as the threshold signal. Average area covered by the immune-positive cells was stated as the percentage of the total area of the area of the frames of interest.

In addition, brains from all groups (n = 4–5 per group) were utilized for computer-aided morphometric analysis. Myelination and axonal enrichment in corpus callosum, cingulum, supragranular layers of somatosensory cerebral cortex (S1) and infragranular layers of motor cortex (M2), and retrosplenial cortex were analysed on these regions of interest (ROI) in sections double immunostained with MBP and NF 200 kDa. In the same areas, the densities of mature oligodendrocytes, identified by their GST-π expression, and of NG2$^+$ oligodendrocyte precursor cells (OPCs) was assessed and expressed as mean value ± SD (Girolamo et al., 2011; Tansey and Cammer, 1991).

Quantitative analysis of Manders' overlap coefficient, an estimate of the fraction of NF$^+$ pixels overlapping the MBP$^+$ pixels in each ROI was performed on confocal single optical plane of double immunolabelled images using JACop plugin of ImageJ (NIH, Bethesda, MD, USA) (Bolte and Cordelieres, 2006).

2.3. Statistical evaluation

All data, where applicable, were expressed as mean ± standard deviation. Statistical significance between the individual groups was tested using one-way analysis of variance (ANOVA), followed by Bonferroni post *hoc* test and the software GraphPad Prism®, Version 5 (GraphPad Software Inc., La Jolla, CA USA). Data on cell density and Manders' coefficient were statistically analyzed using ANOVA followed by Newman-Keuls post *hoc* test for pairwise comparison, using GraphPad Prism 5.04 (GraphPad Software, Inc., La Jolla, CA, USA). A p value of ≤ 0.05 was considered significant.

3. Results

3.1. LD_{50} of MIMO2

Percentage mortality observed was varied with the different doses of MIMO2 administered. Mortality was recorded as $(\frac{number\ dead}{total\ number})$. Mortalities were recorded as number of deceased mice and days (D) of these events:

MIMO2 100 mg - D2 ($^1/_4$), D3 ($^2/_4$), D5 ($^3/_4$).
MIMO2 75 mg/kg – D1 ($^2/_4$), D3 ($^4/_4$).
MIMO2 50 mg/kg – D3 ($^1/_4$).
MIMO2 25 mg/kg – No mortality recorded (Fig. 1)

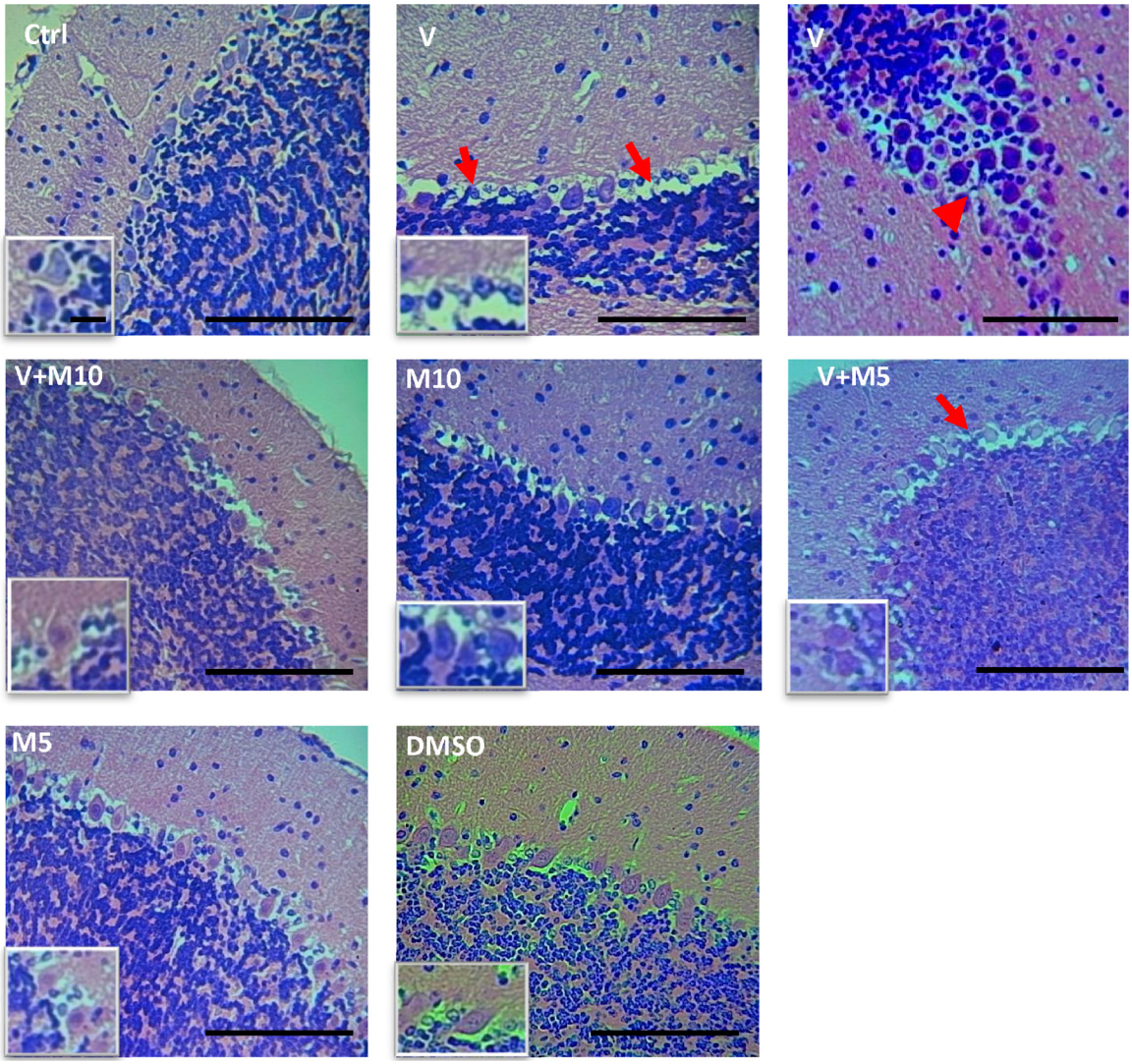

Fig. 6. Micrographs of the cerebellum of treated mice, H&E stain. Note the differing appearances of the Purkinje cells (arrows) in all the groups, the pyknotic appearance, loss of Purkinje cells and also loss of dendritic arborisation in V and M5 + V groups. Note Purkinje layer stratification in V micrograph (upper row, right, red arrowhead). Insets are magnification of the Purkinje cell layer in each group. Groups – Ctrl (sterile H_2O – control); V (Vanadium 3 mg/kg); V + M10 (Vanadium 3 mg/kg + MIMO2 10 mg/kg); M10 (MIMO2 10 mg/kg); M5 (MIMO2 5 mg/kg); V + M5 (Vanadium 3 mg/kg + MIMO2 5 mg/kg); DMSO: dimethyl sulphoxide. Scale bar = 50 μm, insets = 8 μm (remains constant for all the micrographs and insets). Number of mice per group = 5.

Using mortality results obtained from the different MIMO2 doses administered, and based on Lorke's formula, dose for MIMO2 was 35 mg/kg.

3.1.1. Vanadium 3 mg/kg used in combination with MIMO2 at different concentrations

The co-administration of vanadium 3 mg/kg (V) with different concentrations of MIMO2 resulted in varied degrees of mortality. The mortality recorded on the different days for the various concentrations were:

V + MIMO2 35 mg/kg – D2 ($^1/_5$), D4 ($^3/_5$), D5 ($^5/_5$)
V + MIMO2 25 mg/kg – D6 ($^3/_4$)
V + MIMO2 15 mg/kg – No mortality recorded
V + MIMO2 10 mg/kg – No mortality recorded (Fig. 2)

3.1.2. Neurobehavioural tests

Hanging Wire Test: Statistically significant difference ($p < 0.05$) was observed between water and the following groups – V, M10, M5, V + M5, with the water control group having the highest value, followed closely by V + M10 group. The V group had the lowest value (Fig. 3).

Open Field Test: M10 group appeared to be the most active group, having the highest values for rearing and line crossings (Fig. 4 A & B). The vanadium group showed the lowest values for these tests (Fig. 4), being statistically significantly lower than the control and V + M10 groups in rearing and line crossing.

3.1.3. Effect of MIMO2 on vanadium induced neurotoxicity in developing mice

3.1.3.1. Effect on body and relative brain weights. Since MIMO2 is fat soluble and would likely have the tendency to accumulate in body fat and supposing the toxicity which may occur in daily administration, it was administered at day 0, after 48 h and every 72 h thereafter (D0, D2, D5, D8, D11, D14) as was done for vit E (Olopade et al., 2011).

Comparing the increase in body weight of the different groups on D13 of treatment compared to D0, statistical analysis using *t*-test only showed a statistically significant difference ($p < 0.05$) between the water control group and vanadium (V) group, with the vanadium group showing a reduction in body weight increase relative to control (Fig. 5A). The relative brain weight values did not show any statistically significant difference across the groups ($p > 0.05$) (Fig. 5B).

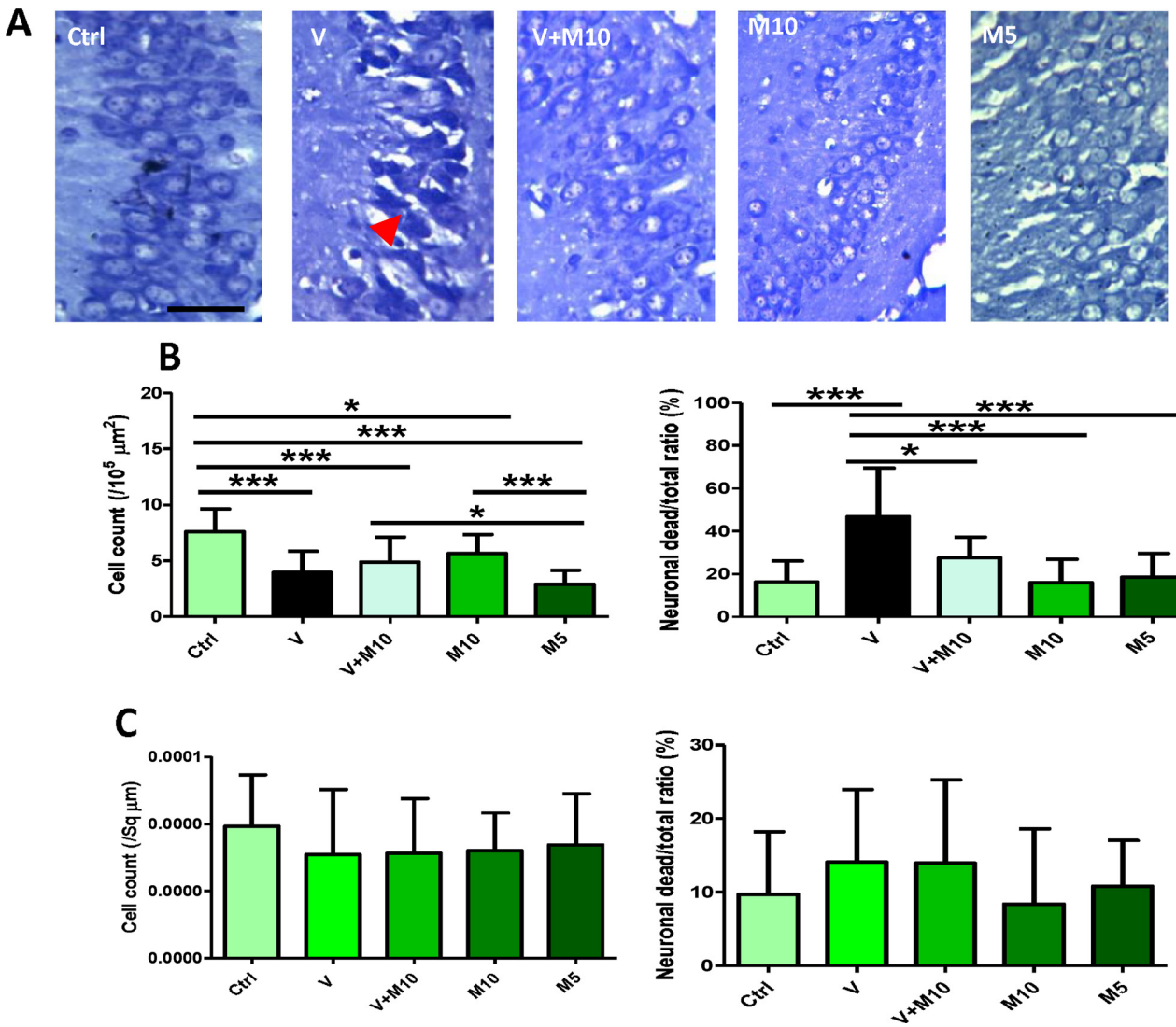

Fig. 7. A shows micrographs of the CA3 region of the hippocampus of treated mice. Note the pyknotic appearance and loss of normal morphology of the cells in the V group (arrowhead). Scale bar = 50 µm, same for all the micrographs. B shows the hippocampal region CA1 cell count. Left chart shows cell count of apparently healthy cells, while right chart shows the cell count of relative number of dead cells expressed in percentage. Number of mice per group = 5. (*$p < 0.05$, **$p < 0.01$, ***$p < 0.001$). C shows the hippocampal region CA3 cell count. Left chart is cell count of apparently healthy cells, while right chart is cell count of relative number of dead cells expressed in percentage. No statistically significant difference was observed amongst the groups. Groups – Ctrl (sterile H_2O – control); V (Vanadium 3 mg/kg); V + M10 (Vanadium 3 mg/kg + MIMO2 10 mg/kg); M10 (MIMO2 10 mg/kg); M5 (MIMO2 5 mg/kg). Number of mice per group = 5.

3.1.4. Histopathology

3.1.4.1. Haematoxylin and eosin. In the cerebellum of the V(vanadium) group, degenerated (pyknotic, with loss of dendritic arborisation) and even loss of Purkinje cells was evident in several areas of different folia (Fig. 6). Also, the granular layer showed a more intense and increased granulation. V + M5 group also showed same pathological features, although not as intense as the vanadium group. In the V group, 80 % (4 out of 5) of the mice showed stratification of the Purkinje cell layer in several areas of different folia, while in V + M10, only 20 % (1 out of 5) showed the stratification in a focal area of folia. The pathological features observed in the cerebellum of the V group were alleviated in the V + M10 group (Fig. 6).

3.1.4.2. Cresyl violet staining. Hippocampal cells of the CA1 and CA3 regions in the V group appeared vacuolated and pyknotic, there was distorted neuronal morphology and loss of nuclear outline (Fig. 7A).

CA1 region: Cell count of apparently healthy cells showed that all experimental groups were affected with respect to the control group ($p < 0.05$). A cell count of apparently normal healthy cells showed a slightly higher value in the V + M10 group when compared with V group, although still not statistically significant ($p > 0.05$; $p = 0.623$). However, cell count of the relative number of dead neurons (expressed in percentage) showed that the vanadium group had the highest number of dead cells, statistically different from all the other experimental groups ($p < 0.05$) (Fig. 7B).

CA3 region: Cell count showed no statistically significant difference ($p > 0.05$) amongst the groups, even though the V group presented the lowest number of cells and the highest number of relative dead cell ratio (Fig. 7C).

Results obtained indicated that M10 gave a better protection than M5, therefore further assays were limited to M10.

3.1.4.3. Histochemistry (black gold II). Major areas assessed for the BGII stain are highlighted in Fig. 8A.

In the V group, BGII histochemistry showed selective demyelination of the corpus callosum (being most pronounced in the middle band, relative to the upper and lower bands), the deeper layers of the retrosplenial and somatosensory cortices, the hippocampus (which was more

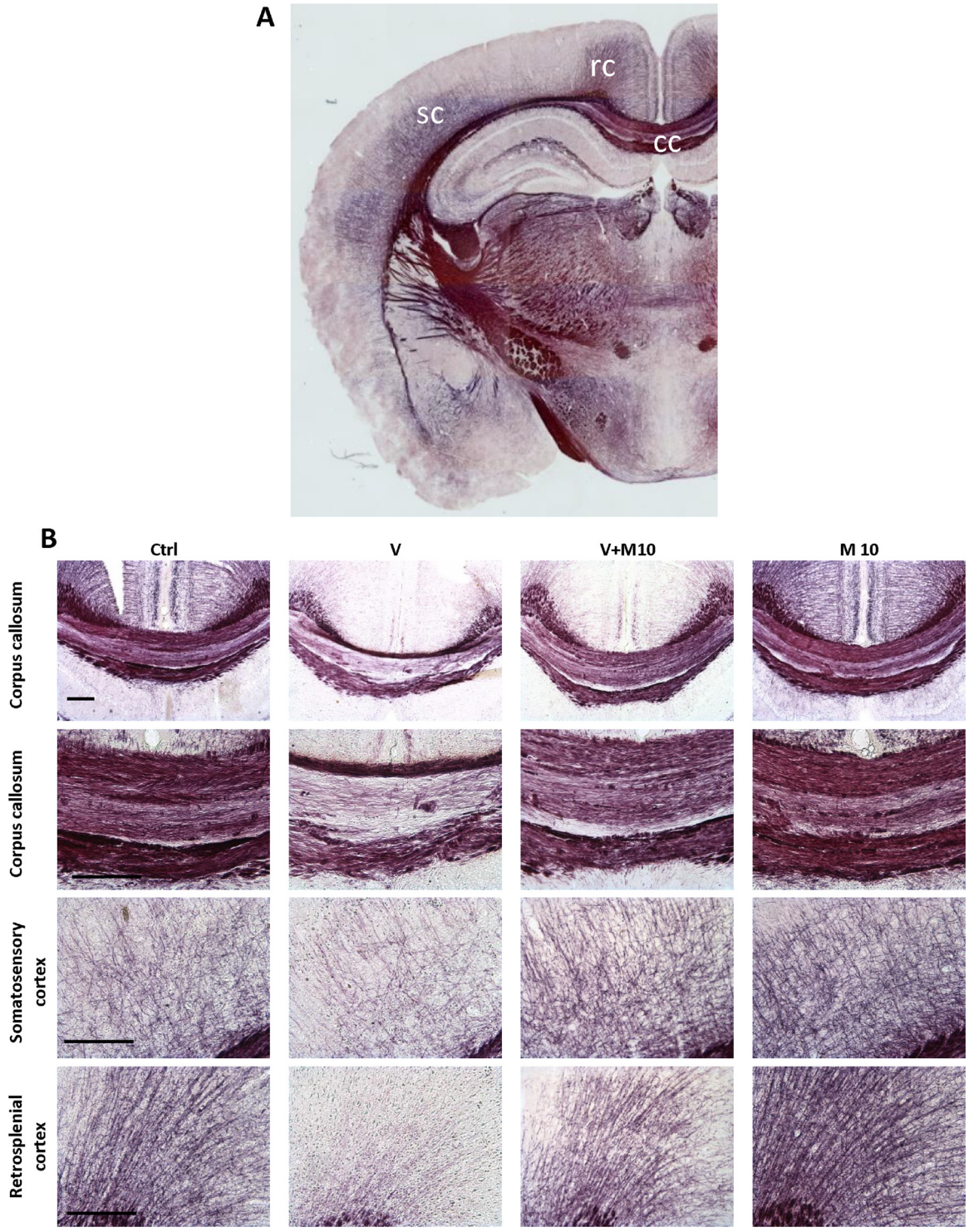

Fig. 8. A is micrograph of whole brain stained with Black gold II. The corpus callosum (cc), somatosensory cortex (sc) and retrosplenial cortex (rc) are labelled. These were the major regions analysed for densitometry. B shows Black gold II histochemistry. Panels show demyelination in the corpus callosum at different magnifications (low magnification – first row; high magnification – second row), deep layers of the somatosensory cortex and the retrosplenial cortex in the vanadium administered group. Note that MIMO2 at 10 mg/kg showed a level of myelin recovery. Scale bar 200 μm (note – scale bar is same across the rows).

pronounced in the CA1 region), the habenular, the region of the thalamus, and the rostral commissure (Fig. 8B and 9A). In the V group, in spite of the severe demyelination observed in the cortices, corpus callosum and the thalamus, the internal capsule appeared relatively resistant to the demyelination (Fig. 9A). The demyelination observed in V group was considerably reduced with the co-administration of M10, in all the brain regions, as seen in the V + M10 group. M10 appeared to have a myelin-potentiating effect, when administered alone (Figs. 8B and 9 A, B).

3.2. Black gold II densitometric analysis (Demyelination)

With administration of vanadium, the brains in group V showed a widespread demyelination, especially in the middle band of the corpus

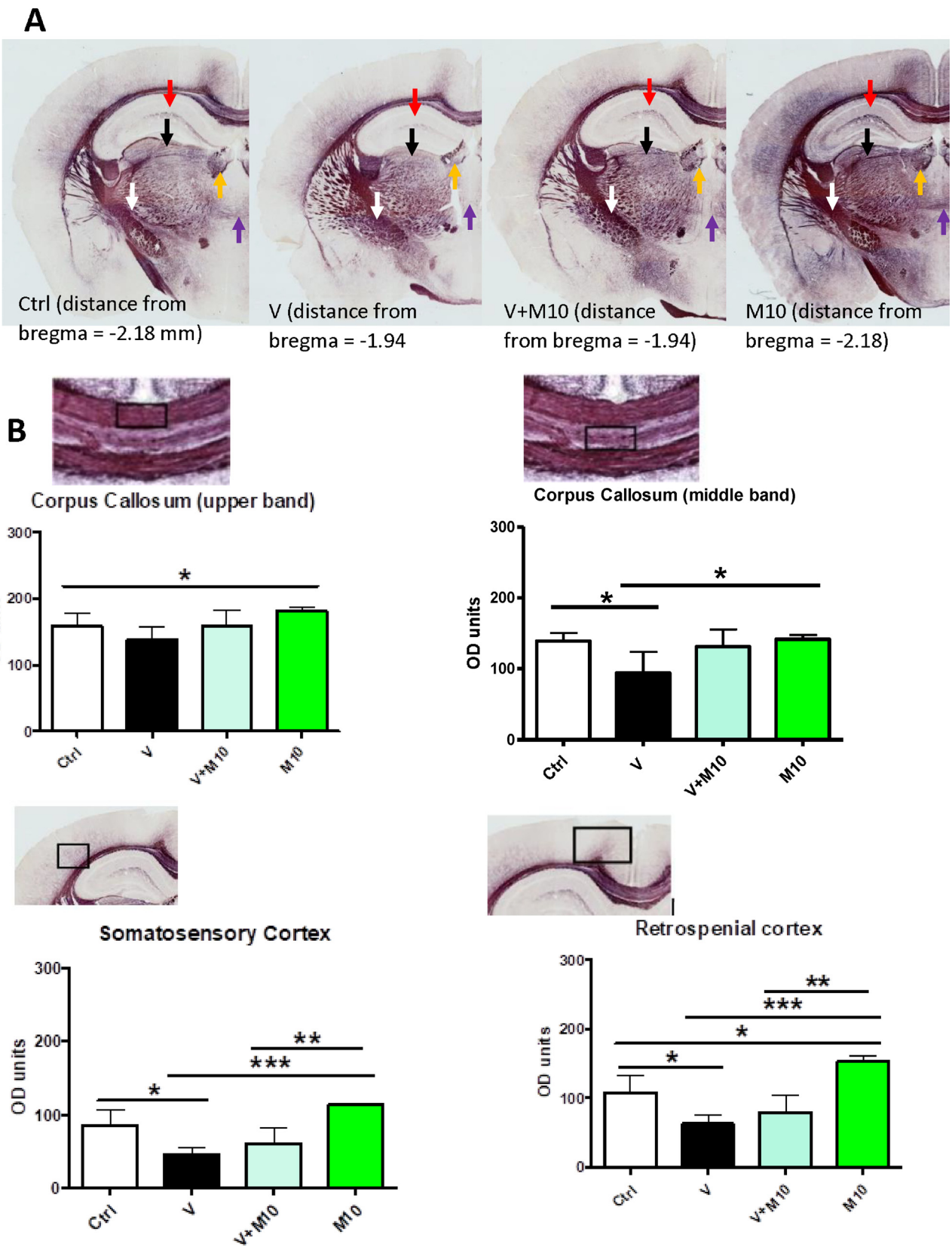

Fig. 9. A is micrographs of whole brain stained with Black gold II, showing demyelination in the CA1 region (red arrow), the thalamus (black arrow), the habenula (yellow arrow) and the rostral commissure (purple arrow). The internal capsule (white arrow) appeared resistant to the demyelination. Distance of each section from the bregma is according to Paxinos and Franklin (2001). B depicts graphs showing the degree of myelination by densitometry of Black Gold II histochemistry expressed as optical density (OD) of the corpus callosum (upper and middle bands), the somatosensory and retrosplenial cortices. Micrographs in B denote the regions of concern (highlighted in a box), all from the control groups. Groups – Control (sterile water); V (Vanadium 3 mg/kg); V + M10 (Vanadium 3 mg/kg + MIMO2 10 mg/kg); M10 (MIMO2 10 mg/kg). Number of mice per group = 5. (*p < 0.05, **p < 0.01, ***p < 0.001).

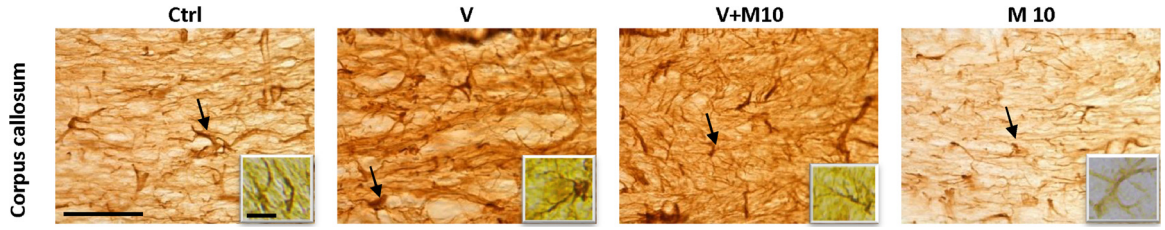

Fig. 10. GFAP immunostaining of the corpus callosum. Note the increased astrocytic activation (bigger cell bodies and increased thickness of their processes) in the vanadium group and the attenuation of astrocyte reactivity observed with the administration of MIMO2. Arrows indicate representative astrocytes. Inset - enlarged individual astrocytes, showing bigger cell bodies in V group relative to other groups. Scale bar = 50 μm, insets = 16 μm (scale bars remain constant for all micrographs and insets).

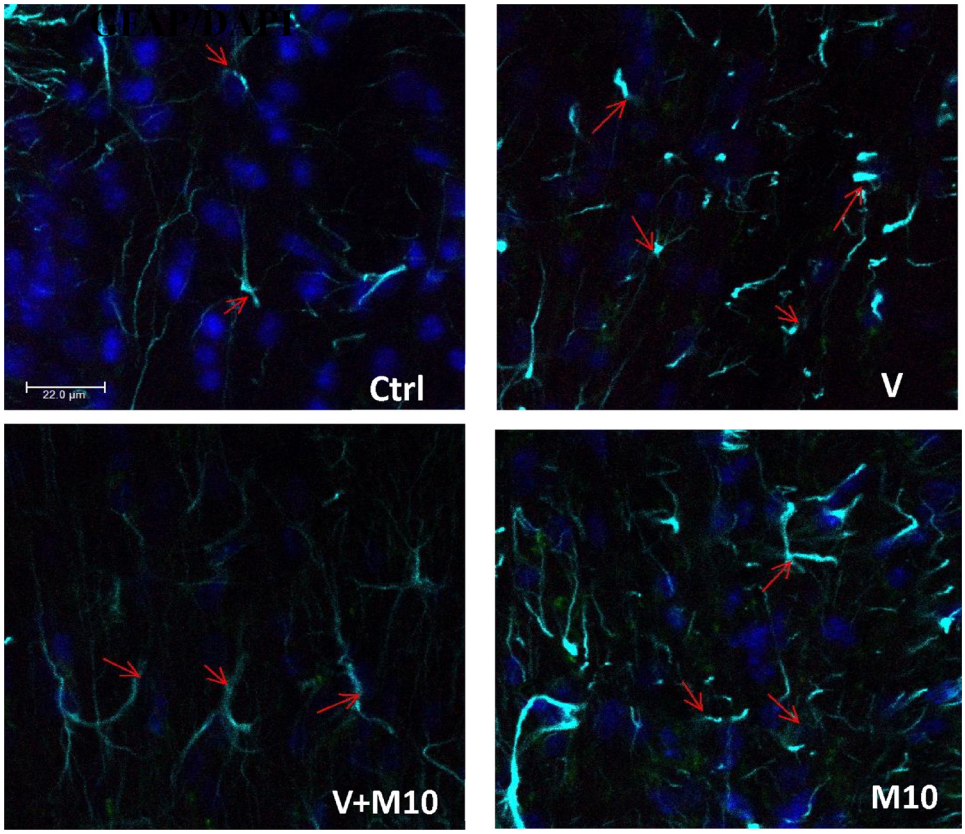

Fig. 11. Representative immunofluorescence/confocal microscopy images of corpus callosum. Note the increase in size of astrocytic cell bodies (arrows) in V group and the amelioration in V + M10 group. Scale bar 22 μm (constant for all micrographs).

callosum, and also evident in the somatosensory and retrosplenial cortices (Figs. 8 and 9). Densitometric analysis revealed statistically significant demyelination ($p < 0.05$) in the middle band of the corpus callosum and the cortices of the V group, and also an amelioration with the co-administration of M10, reverting to the control group value. Densitometric analysis of the corpus callosum upper band and the cortices confirmed that the myelination density of the M10 group was higher than control group (Fig. 9B).

3.3. Glial fibrillary acidic protein - GFAP (astrocytes)

Qualitative evaluation showed greater astrocytic activation in the V group, which appeared to be alleviated with the co-administration of M10. Astrocytic activation was evidenced by the bigger cell bodies and thicker processes. Astrocytic activation was not observed in the M10 group (Figs. 10 and 11). Analysis by immunoperoxidase and immunofluorescence revealed the same results.

3.4. Iba1 immunohistochemistry (microglia)

Microglial activation was observed in the corpus callosum, somatosensory and retrosplenial cortices of the V group. The microglia showed bigger soma, and an increased density than control. The biggest somata were seen in the corpus callosum. M10 group showed higher number of microglia relative to the control group, although this was not significantly different ($p > 0.05$). The use of M10 in combination with vanadium showed a significant reduction in microglia activation relative to the group administered vanadium alone (V group). (Fig. 12A and B).

3.5. Oligodendrocyte lineage cells

3.5.1. Mature oligodendrocytes

On the basis of the observed demyelination of the corpus callosum of vanadium-treated mice, we investigated the expression of the pi form of glutathione-S-transferase (GST-π), which specifically localizes in mature oligodendrocyte cell bodies and mildly in their myelin-forming

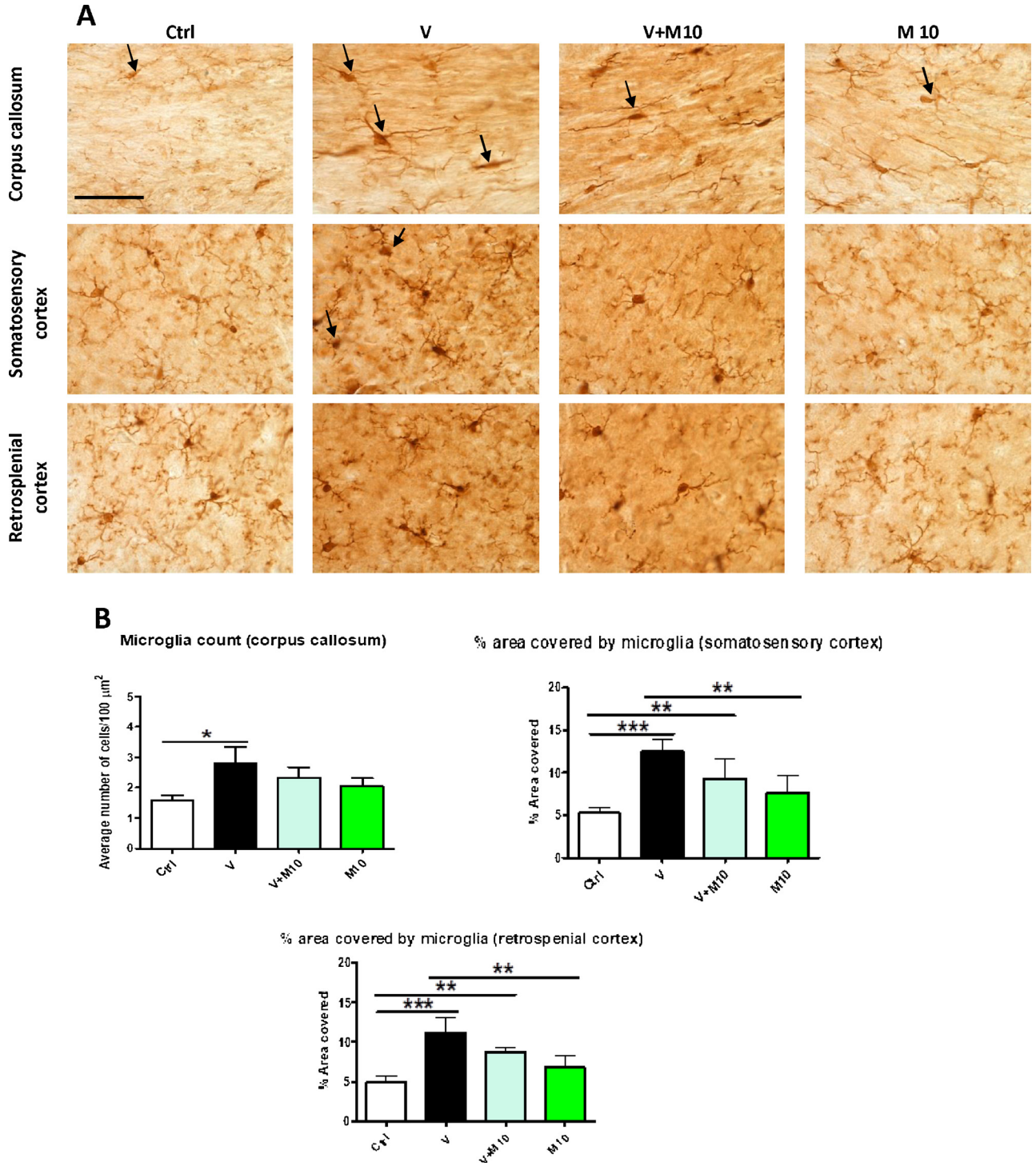

Fig. 12. A is Iba1 immunostaining, showing microglia in the corpus callosum, somatosensory and retrosplenial cortices. In the vanadium group, note the increase in the number of the microglia, and the bigger cell body. Scale bar = 50 µm (constant for all micrographs). B are the graphs showing the Iba1$^+$ microglia counting in the corpus callosum, and Iba1$^+$ percentage area covered in the cortices. Groups – Ctrl (water); V (Vanadium 3 mg/kg); V + M10 (Vanadium 3 mg/kg + MIMO2 10 mg/kg); M10(MIMO2 10 mg/kg). Number of mice per group = 5. (*p < 0.05, **p < 0.01, ***p < 0.001).

processes in adult mouse brain (Girolamo et al., 2011; Tansey and Cammer, 1991). Decreased GST-π staining of oligodendrocytes was appreciated in vanadium-treated mice, especially in the corpus callosum and cingulum white matter regions. Quantification of GST-π$^+$ oligodendrocyte density (number of positive cells/10^6 µm^3 of ROI volume) confirmed the qualitative observations of mature oligodendrocytes reduction in the corpus callosum of V treated group compared to controls. The GST-π$^+$ oligodendrocyte density of cingulum appeared not significantly reduced despite the observed weaker GST-π immunolabelling of this ROI in vanadium-treated mice.

M10 treatment rescued vanadium-induced damage, as a regaining of control level of GST + mature oligodendrocyte density was observed (Figs. 13 and 14). In this analysis, as in the analyses of the following markers, M10 treatment alone (M10 group) *per se* did not show significant variations with respect to control mice (Figs. 13,14,16,18).

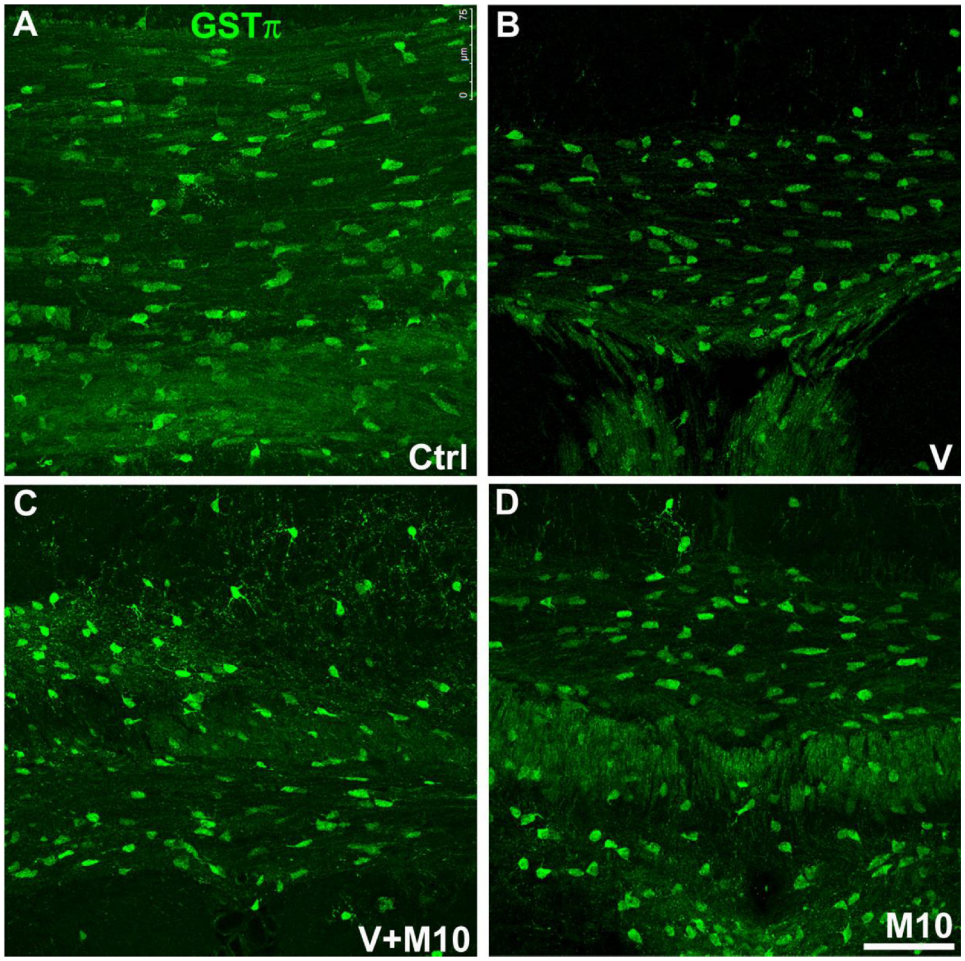

Fig. 13. Representative confocal images of the corpus callosum immunolabelled with GST-π positive mature oligodendrocytes. (A) control (B) vanadium (C) V + M10 (D) M10 treated mice. Scale bar: 75 μm.

3.6. Myelinated axons

Myelin damage appeared as regional loss of MBP staining especially evident in middle band of midsagittal portion of corpus callosum, in cingulum and in primary somatosensory cortex of V-treated mice compared to controls (Fig. 15A–D). The quantitative assessment of myelinated axons was based on the evaluation of the MBP overlap of NF immunofluorescence (Manders' coefficient) (Fig. 15). After vanadium exposure, a significant reduction of such overlap was found in all the sampled regions (with the only exception of cortical infragranular layers of M2 cortex) (Fig. 16A–D). This alteration was reverted when vanadium exposure had been combined with M10 treatment (Fig. 16A–D).

3.6.1. Oligodendrocyte precursor cells

Oligodendrocyte precursor cells (OPCs) were identified by NG2 (nerve-glial antigen 2) chondroitin sulphate proteoglycan expression, molecule involved in proliferation and cell migration during development, adulthood and after injury and were considered a potential source of myelin-regenerating oligodendrocytes (Di Bello et al., 1999; Girolamo et al., 2011; Tripathi et al., 2010). In all the analyzed brain regions of V-treated mice, OPCs appeared hypertrophic, with bushy, more ramified appearance and increased NG2 immunolabelling, compared to control mice (Fig. 17). The distribution of hypertrophic NG2+ OPCs closely correspond to the observed demyelinated areas, as described in commissural midline portion of the corpus callosum, cingulum, and cerebral cortex S1 and M2 (Fig. 15). Supporting these observations, the quantitative analysis of NG2-positive OPCs showed a significant increase in the density of these cells after vanadium exposure with respect to controls throughout the sampled regions (Fig. 18). This effect was completely reversed in the group in which vanadium exposure had been combined with M10 treatment in the examined regions, (Fig. 18).

4. Discussion

There has been an increase in the awareness and use of plants as a means of treating different ailments and diseases. Economic recession, most especially in the developing countries, will cause an increase in the quest for local and more affordable alternatives to orthodox medicine. *Moringa oleifera* leaves (MOL) in the form of various extracts have been used by different Authors to treat a number of neurotoxic, neurodegenerative and related conditions in laboratory animals (Mohan et al., 2005; Singh et al., 2012; Sutalangka et al., 2013; Kirisattayakul et al., 2012, 2013). The positive effect experienced by different Authors could be attributable to the fact that the leaves contain a high level of polyphenols and other antioxidants which cause neuroprotection by either scavenging free radicals or activating cellular antioxidative system or both (Luqman et al., 2012).

The increase in use of MOL for different disease conditions has made it imperative to isolate the active agent in the plant to improve the possible results obtainable. As of the time of submission of this manuscript, this is probably the first report of using a pure compound (with a well-defined structure) isolated from MOL to treat vanadium-induced neurodegeneration in a laboratory animal.

MIMO2 was a compound shown to be fat soluble and not water

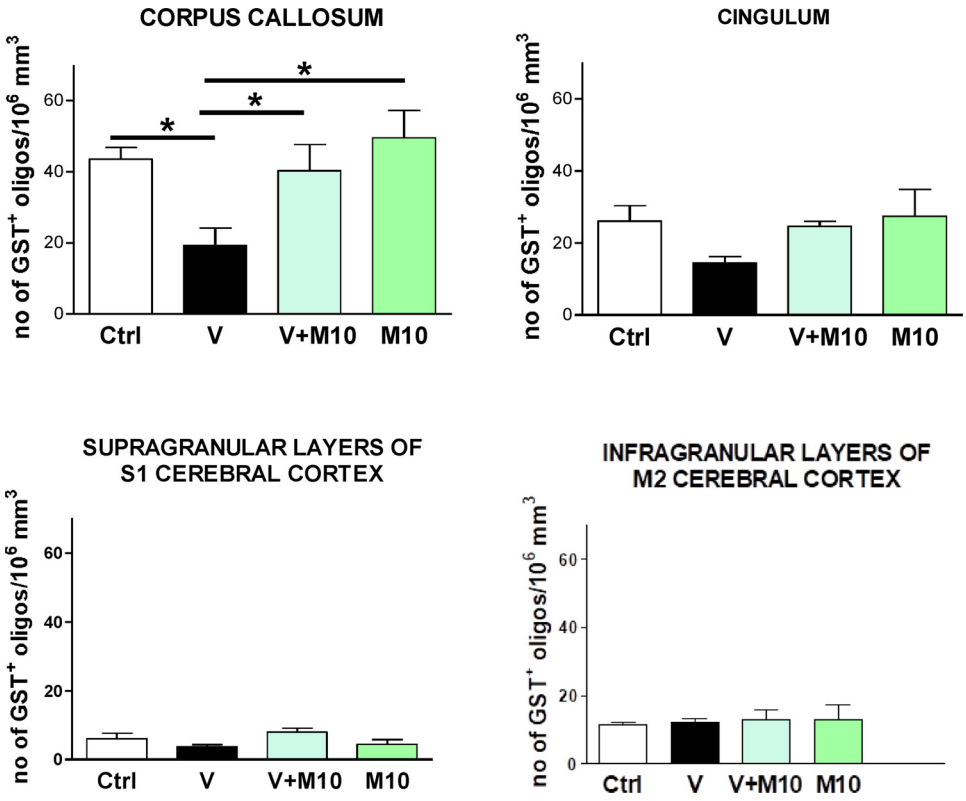

Fig. 14. Quantitative analysis of the number of GST-π positive mature oligodendrocytes in corpus callosum (A), cingulum (B), cerebral cortex supragranular layers (C) and infragranular layers (D), of control (Ctrl), vanadium (V), vanadium + M10 (V + M10) and M10 treated mice. One-way ANOVA with Newman-Keuls post hoc test, *$p < 0.05$, **$p < 0.01$ and ***$p < 0.001$. The error bars are SD. Groups – Ctrl (water); V (Vanadium 3 mg/kg); V + M10 (Vanadium 3 mg/kg + MIMO2 10 mg/kg); M10 (MIMO2 10 mg/kg). Number of mice per group = 5.

soluble. This property may imply that it has the tendency to accumulate in the body and may cause lipid peroxidation at high doses, instead of reducing it, as was reported in vitamin E (Salonen et al., 2000). In this case, it was advisable to give MIMO2 at staggered doses. Giving MIMO2 25 mg/kg alone recorded 100 % survival of the treated mice, while using the same dose in combination with vanadium resulted in mortality. This suggests that the two drugs had a potentiating effect (pro-oxidant) on each other, thereby resulting in increased mortality/morbidity when combined at these doses.

4.1. Body weight and functional deficit

Body weight and relative brain weight did not show any significant difference relative to the control and V 3 mg groups. This is in contrast to what was reported by Mustapha et al. (2014) and Azeez et al. (2016). This could be attributed to the fact that in the aforementioned experiments, vanadium administration commenced from post-natal day 1 (PND1), while in the current experiment, it commenced on PND14. The age of exposure of the pups probably played a very important role in their response to insults.

The present findings show that vanadium administration starting from PND 14 may not significantly affect the weight gain but resulted in a decrease in locomotion and exploratory activity.

The finding in this study of no significant difference in the body weight increase across the groups is similar to reports by García et al. (2004, 2005) and Igado et al. (2012), who exposed to a 5 days-treatment of vanadium 3-month-old rats and 2-month-old rats, respectively. Contrary to these obtained results were the experiments by Azeez et al. (2016), who reported a significant decrease in body weight with vanadium administration to mice for 90 days, *via* lactating dam and through the intraperitoneal route. It could be deduced from this result that the effect of vanadium administration on body weight may not only be related to the duration, but also to the age at commencement of administration. It is however possible that dosing for a longer period in the current study may result in a statistically significant difference.

Addition of M10 to vanadium showed a significant alleviation of the muscular weakness observed in the V alone group. Significant decreased muscular strength (*hanging wire test)* and locomotion (*open field test*) relative to the control group was observed in V, M10 mg/kg, M5 mg/kg and V + M5. Administration of vanadium has previously been reported to result in muscular weakness in mice (Azeez et al., 2016; Mustapha et al., 2014). There was a significant increase in rearing and line crossing in the M10 mg/kg, implying that the animals in this group were more excitable. It should however be noted that the administration of MIMO2 at a dose that alleviated the vanadium neurotoxicity may be toxic when used alone, giving pro-oxidative effects, similar to that observed in α-tocopherol and *Garcinia kola* (Abudu et al., 2004; Igado et al., 2012).

4.2. Purkinje layer stratification and loss of Purkinje cells

Stratification of the Purkinje layer is observed in migrating cells in the developing embryo (Yuasa et al., 1991). The presence of the stratification of Purkinje neurons in the V-treated groups could be due to the vanadium effect on cell migration as similarly reported in the case of lead poisoning in mice (Jaarsma et al., 2014). This was less evident in the group co-administered with vanadium and M10. The observed pyknosis of the cerebellar neurons is consistent with previous reports by Igado et al. (2012), where vanadium has been reported to result in neuronal cell death, or a decrease in neuronal cell population. The pathologic features observed in the cerebellum of the vanadium treated group could partially account for the relative muscle weakness, since the cerebellum is responsible for muscle coordination (Afifi and Bergman, 2005a). Previous reports of Purkinje cell stratification have been documented in lead poisonings in mice and in Bicaudal-D protein knockout mice (Jaarsma et al., 2014). However, to the best of our knowledge, this current study is the first report of vanadium administration resulting in Purkinje cell stratification.

4.3. Hippocampal neuronal count

The effect of vanadium on the hippocampal neuronal cells is similar

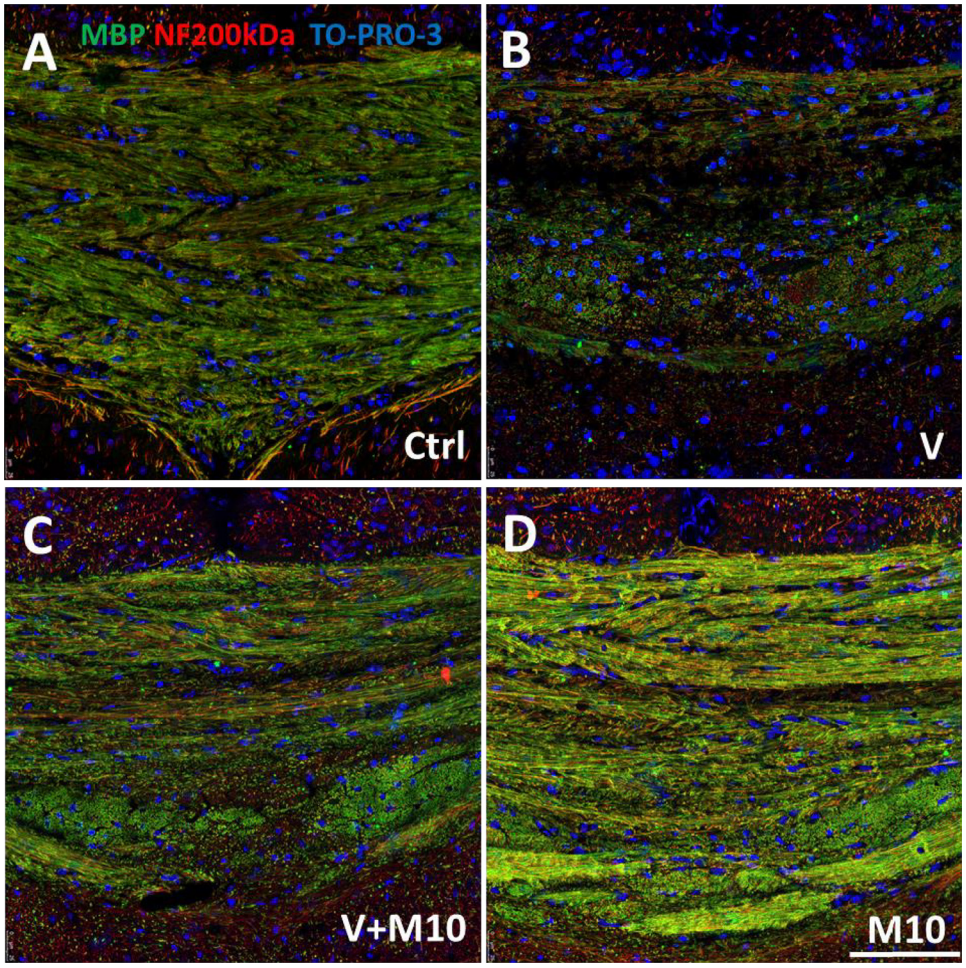

Fig. 15. Representative confocal images of corpus callosum immunolabelled with anti-MBP and anti-NF200 kDa (A) control (B) vanadium (C) V + M10 (D) M10 treated mice. Scale bar: 75 μm.

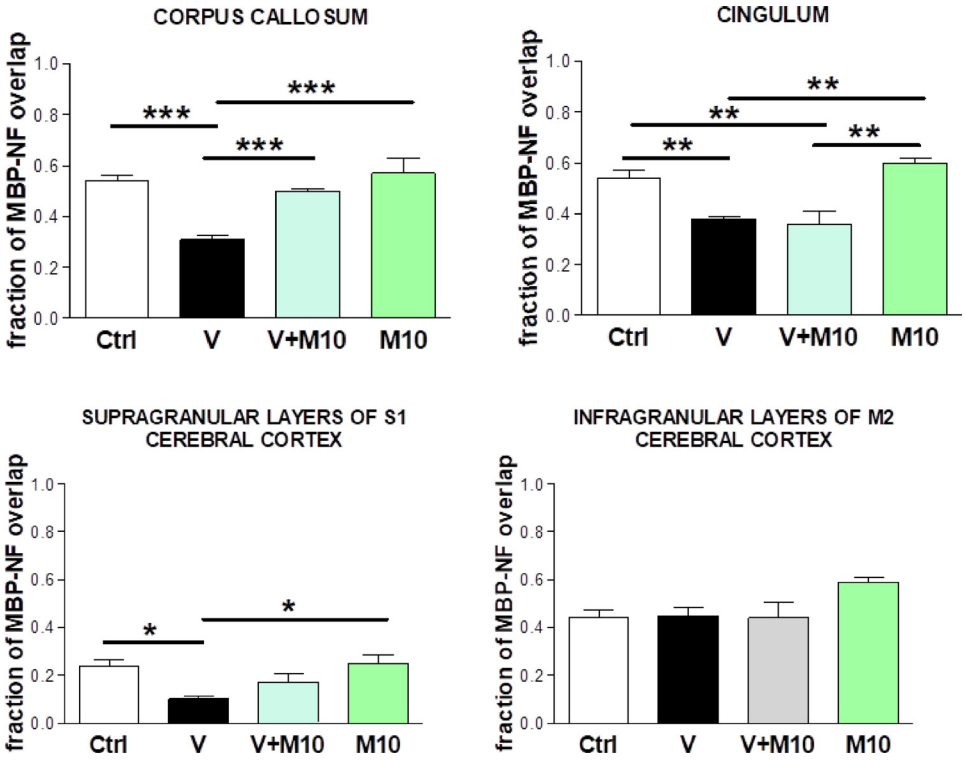

Fig. 16. Quantitative analysis of overlap (Manders' coefficient) of MBP (myelin) on NF200 kDa (axon) in corpus callosum (A), cingulum (B), cerebral cortex supragranular layers (C). and infragranular layers (D) of control (Ctrl), vanadium (V), vanadium + M10 (V + M10) and M10 treated mice. One-way ANOVA with Newman-Keuls post hoc test, *$p < 0.05$, **$p < 0.01$ and ***$p < 0.001$. Groups – Ctrl (water); V (Vanadium 3 mg/kg); V + M10 (Vanadium 3 mg/kg + MIMO2 10 mg/kg); M10 (MIMO2 10 mg/kg). Number of mice per group = 5.

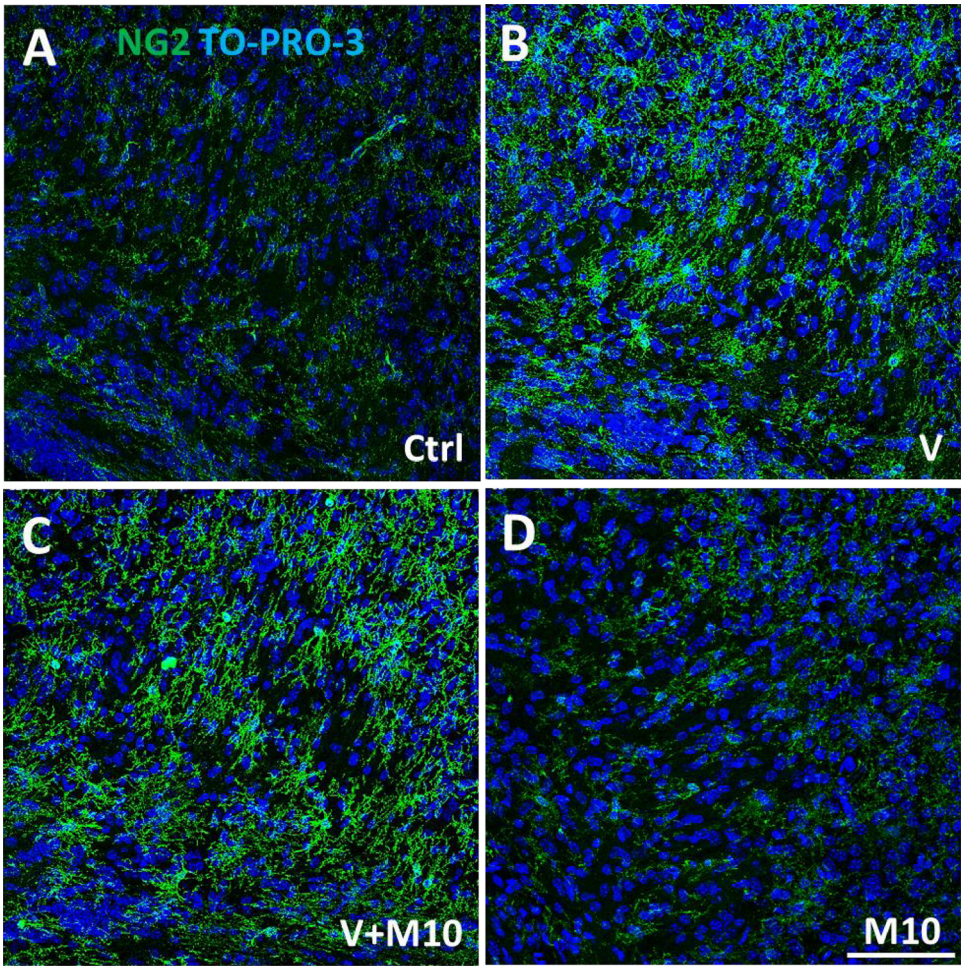

Fig. 17. Representative confocal microscopy image of cingulum immunolabelled for NG2+ OPCs of (A) control, (B) vanadium, (C) V + M10, (D) M10 treated mice. Scale bar: 75 μm.

to that observed by Sutalangka et al. (2013), when he induced dementia with a cholinotoxin. He reported an ameliorative effect caused by the oral administration of the hydroalcohol extract of *Moringa oleifera* leaves. The effect of MIMO2 on the cells however, appeared to be stronger if compared to what was observed with the administration of the leave extract.

The CA1 region was more susceptible to vanadium-induced damage relative to the CA3. This could be due to the fact that the CA3 region is documented to be the hippocampal region that is the least susceptible to insults (Afifi et al., 2005b).

4.4. Demyelination

Demyelination or hypomyelination has been reported in vanadium exposure, *via* lactation or direct intraperitoneal injection (Igado et al., 2012; Mustapha et al., 2014). The highest lipid content of the brain is in the myelin. The high metabolic activity of myelin increases the vulnerability of nervous tissue to peroxidase damage. Vanadium causes lipid peroxidation in different regions of the brain, resulting in an initiation of oxidative chain reactions. Because myelin possesses a high relative content of phospholipids, it becomes a potential target for V-induced membrane oxidative damage (García et al., 2004; Igado et al., 2012). Histopathological analysis of vanadium-treated brains revealed demyelination in a region-dependent manner. Activation of astrocytes and microglia was consistent with demyelination observed. Demyelination in this study was observed mainly in the midline of the corpus callosum, the hippocampus, and diencephalon. This region-selective demyelination is similar to that reported in cuprizone neurotoxicity (Kipp et al., 2009; Zendedel et al., 2013). Damage to the corpus callosum has been reported to cause subtle changes in bilateral sensory and motor coordination (Berlucchi, 2012). This demyelination effect of vanadium and the alleviation resulting from the use of M10, is mirrored in the results of the hanging wire neurobehavioural test.

The central portion of the corpus callosum commissure has been reported to be vulnerable to toxic challenges probably due to the penetration of toxic agents and arrangement of vascularisation (Berlucchi, 2012). Vanadium crosses the blood brain barrier (Igado et al., 2012), thereby making it easy to cause damage in the brain. The amelioration of demyelination by MIMO2could probably be because it mops up the free radicals produced by the action of vanadium. Probably, it prevents the penetration and action of vanadium, by a mechanism of action that still needs to be further investigated. However, polyphenolic compounds (like MIMO2) exhibit strong antioxidant and anti-inflammatory activities which may lessen or reduce neurodegeneration (Choi et al., 2012; Girolamo et al., 2017). It is also noteworthy, the fact that MIMO2 alone (M10) appeared to potentiate/stimulate the production of myelin. This increased myelin in the corpus callosum and the cortices examined (somatosensory and retrosplenial) could have been responsible for the increased activity observed in the open field and hanging wire tests thereby resulting in improved motor coordination.

Although statistical analysis at $p = 0.05$ did not show statistically significant difference for assessment of myelination using BGII between the V and V + M10 groups (Fig. 9B), immunofluorescence to detect myelinated axons (Fig. 16) showed a statistically significant difference

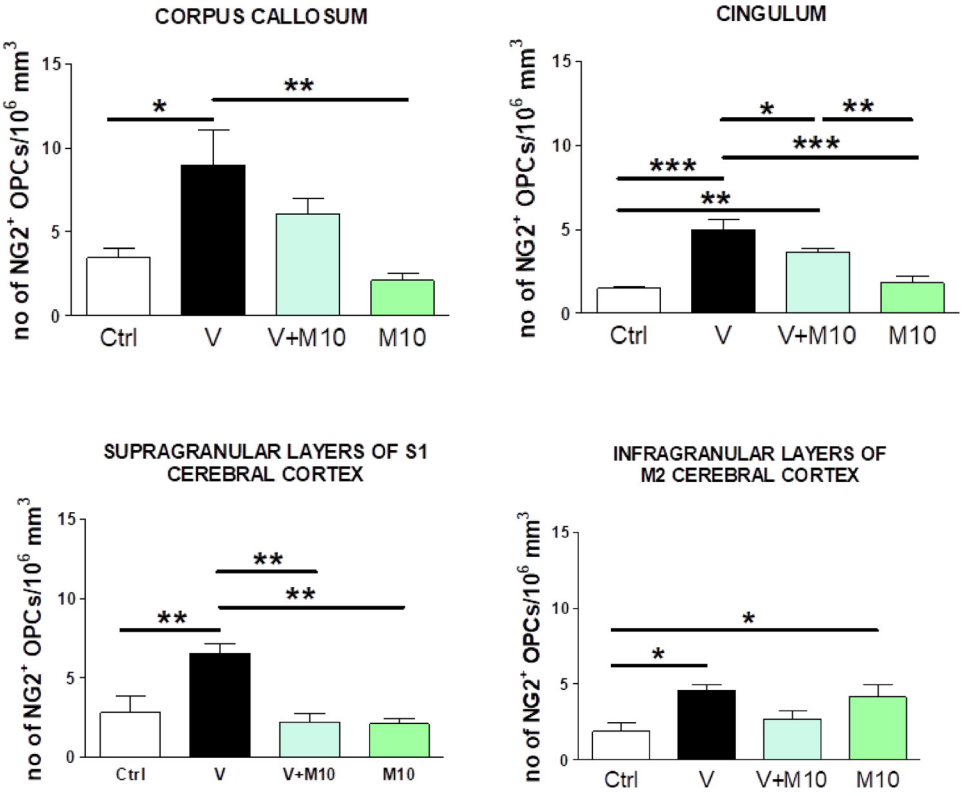

Fig. 18. Quantitative analysis of the number of NG2-positive OPcs in corpus callosum (A), cingulum (B), cerebral cortex supragranular layers (C), and infragranular layers (D) of control (Ctrl), vanadium (V), vanadium + M10 (V + M10) and M10 treated mice. One-way ANOVA with Newman-Keuls post hoc test, *p < 0.05; **p < 0.01; ***p < 0.001. The error bars are SD. Groups – Ctrl (water); V (Vanadium 3 mg/kg); V + M10 (Vanadium 3 mg/kg + MIMO2 10 mg/kg); M10(MIMO2 10 mg/kg). Number of mice per group = 5.

between these groups. This might be because the immunofluorescence is a more sensitive test. It must however be emphasized that the visual difference in the two groups using BGII was distinct.

4.5. Microglia and astrocyte activation

Microglia activation and astrogliosis are characteristic features of CNS lesions (Gudi et al., 2014).

Microglia are resident immunocompetent cells present in the brain parenchyma; they are key mediators of neuroinflammation (Hanisch and Kettenmann, 2007). Microglia activation has been reported to precede demyelination and persist in chronic myelin lesions (Gudi et al., 2014). In this study, although relatively acute compared to the study by Azeez et al. (2016), it was observed that there was a significant increase in microglia activation in all the three brain regions sampled, while significant alleviation was observed in the cortices of V + M10 group examined. This shows that in the corpus callosum, even with the significant amelioration of demyelination, there was not a corresponding decrease in microglia activation.

Recruitment of microglia is reportedly regulated by astrocytes (Gudi et al., 2014; Skripuletz et al., 2013). Astrocytes provide trophic support to other cells and also exert an inhibitory effect on remyelination (Alizadeh et al., 2015). Astrogliosis due to vanadium administration, in different time frames, and in different brain regions have been reported by different authors (Azeez et al., 2016; Garcia et al., 2005). In the current study, immunofluorescence confirmed that astrogliosis was most pronounced in the corpus callosum. This is contrary to what was previously reported by Azeez et al. (2016), where astrogliosis was pronounced in both grey and white matter. The reason for this could be due to the shorter period of exposure in the current study.

4.6. Conclusion

Vanadium administration seemed to show a widespread damage on the brain while MIMO2 consistently showed the ability to decrease the toxicity signs exhibited by vanadium probably due to its antioxidative property. MIMO2 at 10 mg/kg appeared to be relatively safe in the animals (mice). MIMO2 was shown to reduce neurobehavioural deficits induced by vanadium, and it offered *in vivo* neuroprotection against neuronal loss, demyelination, astrocytosis and microglia activation (Fig. 19). This work showed evidence that MIMO2 can stimulate/potentiate myelin production. However, considering that the use of MIMO2 has not been previously documented, further experiments may be required to ascertain a dose that is safe when used alone. This dose may necessarily be different from what is used in combination with a toxicant, as a high dose when used alone (in the absence of a toxicant) may give pro-oxidative effects.

Environmental pollution and its ravages on human and animal system are an ongoing scourge that is on the increase. It is hoped that on the long run, results from this experiments and subsequent studies regarding MIMO2 as a potential drug/food additive will open up vistas to alleviate the ravages of environmental pollution in the form of vanadium-induced neurotoxicity.

Credit author statement

Olumayowa Igado – Animal experimentation, histopathology, immunohistochemistry, discovery, synthesis and production of MIMO2, first draft of manuscript and editing; **Anna Andrioli**, **Idris Azeez** and **Marina Bentivoglio** – immunohistochemistry, immunofluorescence, manuscript draft and editing; **Francesco Girolamo** – immunofluorescence, histopathology, manuscript editing; **Idris Azeez** and **Mariella Errede** - immunofluorescence and histopathology; **Oluwasanmi Aina** – haematoxylin-eosin and cresyl violet histopathology; **Jan Glaser** and **Ulrike Holzgrabe** – discovery, synthesis and production of MIMO2; **James Olopade** – research conceptualisation, manuscript draft and editing.

All authors approved of the final draft of manuscript.

Funding

This work was partly supported by the FUR funds of the University

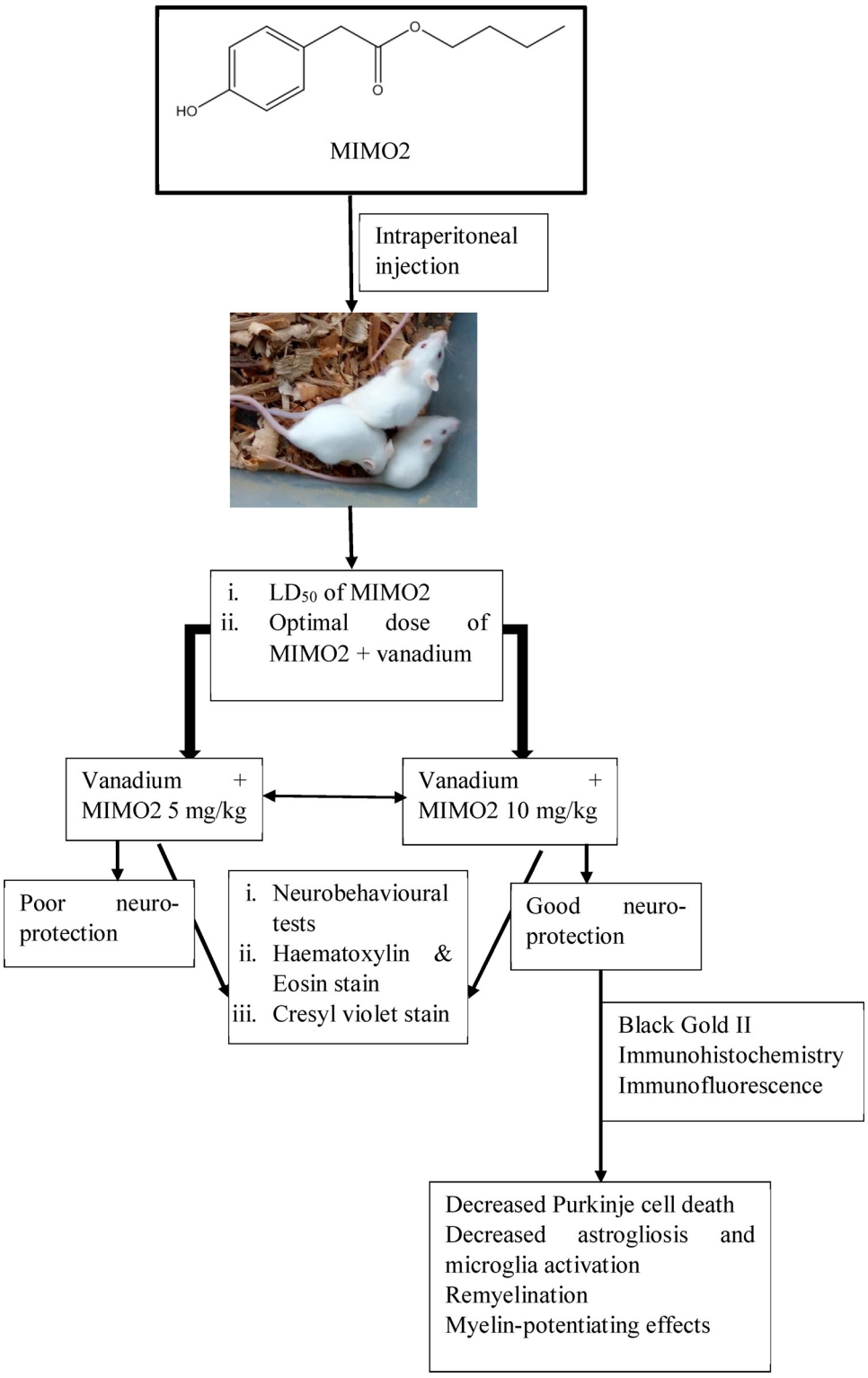

Fig. 19. Flowchart summarising the whole experiment and the neuroprotective effect of MIMO2 in vanadium-induced neurotoxicity in mice.

of Verona, Italy to MB; International Brain research organisation (IBRO) Return Home grant to JOO; Tertiary Education Trust Fund (TETFUND) Nigeria to JOO and OOI

Declaration of Competing Interest

The authors report no declarations of interest.

Acknowledgements

The authors gratefully acknowledge Drs A.A. Obasa and F.A. OlaOlorun, both of the Department of Veterinary Anatomy, University of Ibadan, for their invaluable help in taking care of the mice prior to sacrifice and during sacrifice.

OOI – Animal experimentation, histopathology, immunohistochemistry, discovery, synthesis and production of MIMO2,

first draft of manuscript; AA, IAA and MB – immunohistochemistry, immunofluorescence, manuscript draft and editing; FG – immunofluorescence, histopathology, manuscript editing; IAA and ME - immunofluorescence and histopathology; OOA – haematoxylin-eosin and cresyl violet histopathology; JG and UH – discovery, synthesis and production of MIMO2; JOO – research conceptualisation, manuscript draft and editing.

All authors approved of the final draft of manuscript.

References

Abudu, N., Miller, J.J., Attaelmannan, M., Levinson, S.S., 2004. Vitamins in human arteriosclerosis with emphasis on vitamin C and vitamin E. Clin. Chim. Acta 339, 11–25.

Afifi, A.K., Bergman, R.A., 2005a. In: Ronald, A. (Ed.), Functional Neuroanatomy: Text and Atlas. Lange Medical Books/McGraw-Hill.

Afifi, A.K., Bergman, R.A., Ronald, A., 2005b. Functional Neuroanatomy: Text and Atlas. Lange Medical Books/McGraw-Hill.

Alizadeh, A., Dyck, S.M., Karimi-Abdolrezaee, S., 2015. Myelin damage and repair in pathologic CNS: challenges and prospects. Front. Mol. Neurosci. https://doi.org/10.3389/fnmol.2015.00035.

Azeez, I.A., Olopade, F., Laperchia, C., Andrioli, A., Scambi, I., Onwuka, S.K., et al., 2016. Regional myelin and axon damage and neuroinflammation in the adult mouse brain after long-term postnatal vanadium exposure. J. Neuropathol. Exp. Neurol. 75. https://doi.org/10.1093/jnen/nlw058.

Bakre, A.G., Aderibigbe, A.O., Ademowo, O.G., 2013. Studies on neuropharmacological profile of ethanol extract of *Moringa oleifera* leaves in mice. J. Ethnopharmacol. 149, 783–789. https://doi.org/10.1016/j.jep.2013.08.006.

Bamishaiye, E.I., Olayemi, F.F., Awagu, E.F., Bamshaiye, O.M., 2011. Proximate and phytochemical composition of *Moringa oleifera* leaves at three stages of maturation. Adv. J. Food Sci. Technol. 3 (4), 233–237. http://maxwellsci.com/print/ajfst/v3-233-237.pdf.

Berlucchi, G., 2012. Frontal callosal disconnection syndromes. Cortex 48, 36–45. https://doi.org/10.1016/j.cortex.2011.04.008.

Bolte, S., Cordelieres, F.P., 2006. A guided tour into subcellular colocalisation analysis in light microscopy. J. Microsc. https://doi.org/10.1111/j.1365-2818.2006.01706.x.

Charan, J., Kantharia, N.D., 2013. How to calculate sample size in animal studies? J. Pharmacol. Pharmacother. 4 (4), 303–306. https://doi.org/10.4103/0976-500X.119726.

Choi, D.-Y., Lee, Y.-J., Hong, J.T., Lee, H.-J., 2012. Antioxidant properties of natural polyphenols and their therapeutic potentials for Alzheimer's disease. Brain Res. Bull. 87, 144–153. https://doi.org/10.1016/j.brainresbull.2011.11.014.

Cui, W., Guo, H., Cui, H., 2015. Vanadium toxicity in the thymic development. Oncotarget 6 (30), 28661–28677. https://doi.org/10.18632/oncotarget.5798.

Di Bello, I.C., Dawson, M.R.L., Levine, J.M., Reynolds, R., 1999. Generation of oligodendroglial progenitors in acute inflammatory demyelinating lesions of the rat brain stem is associated with demyelination rather than inflammation. J. Neurocytol. 28, 365–381. https://doi.org/10.1023/A:1007069815302.

Drickamer, L.C., 1981. Selection for age of sexual maturation in mice and the consequences for population regulation. Behav. Neural Biol. 31 (1), 82–89. https://doi.org/10.1016/50163-1047(81)91114-91116.

Englert, N., 2004. Fine particles and human health – a review of epidemiological studies. Toxicol. Lett. 149 (1–3), 235–242. https://doi.org/10.1016/j.toxlet.2003.12.035.

Galuppo, M., Giacoppo, S., De Nicola, G.R., Iori, R., Navarra, M., Lombardo, G.E., Bramanti, P., Mazzon, E., 2014. Antiinflammatory activity of glucomoringin isothiocyanate in a mouse model of experimental autoimmune encephalomyelitis. Fitoterapia 95, 160–174. https://doi.org/10.1016/j.fitote.2014.03.018.

Garcia, G.B., Biancardi, M.E., Quiroga, A.D., 2005. Vanadium (V)-Induced neurotoxicity in the rat central nervous system: a histo-immunohistochemical study. Drug Chem. Toxicol. 28, 329–344. https://doi.org/10.1081/DCT-200064496.

García, G.B., Quiroga, A.D., Stürtz, N., Martinez, A.I., Biancardi, M.E., 2004. Morphological alterations of central nervous system (CNS) myelin in vanadium (V)-exposed adult rats. Drug Chem. Toxicol. 27, 281–293. https://doi.org/10.1081/DCT-120037747.

Giacoppo, S., Galuppo, M., Montaut, S., Iori, R., Rollin, P., Bramanti, P., Mazzon, E., 2015. An overview on neuroprotective effects of isothiocyanates for the treatment of neurodegenerative diseases. Fitoterapia 106, 12–21. https://doi.org/10.1016/j.fitote.2015.08.001.

Girolamo, F., Ferrara, G., Strippoli, M., Rizzi, M., Errede, M., Trojano, M., et al., 2011. Cerebral cortex demyelination and oligodendrocyte precursor response to experimental autoimmune encephalomyelitis. Neurobiol. Dis. https://doi.org/10.1016/j.nbd.2011.05.021.

Girolamo, F., Coppola, C., Ribatti, D., 2017. Immunoregulatory effect of mast cells influenced by microbes in neurodegenerative diseases. Brain Behav. Immun. 65, 68–89. https://doi.org/10.1016/j.bbi.2017.06.017.

Gudi, V., Gingele, S., Skripuletz, T., Stangel, M., 2014. Glial response during cuprizone-induced de- and remyelination in the CNS: lessons learned. Front. Cell. Neurosci. 8, 73. https://doi.org/10.3389/fncel.2014.00073.

Hanisch, U.K., Kettenmann, H., 2007. Microglia: active sensor and versatile effector cells in the normal and pathologic brain. Nat. Neurosci. 10, 1387–1394. https://doi.org/10.1038/nn1997.

Hannan, A., Kang, J., Mohibbullah, M., Hong, Y., Lee, H., Choi, J., Choi, I., Moon, S., 2014. *Moringa oleifera* with promising neuronal survival and neurite outgrowth promoting potentials. J. Ethnopharmacol. 152, 142–150. https://doi.org/10.1016/j.jep.2013.12.036.

Igado, O.O., Olopade, J.O., Adesida, A., Aina, O.O., Farombi, E.O., 2012. Morphological and biochemical investigation into the possible neuroprotective effects of kolaviron (*Garcinia* kola bioflavonoid) on the brains of rats exposed to vanadium. Drug Chem. Toxicol. 35, 371–380. https://doi.org/10.3109/01480545.2011.630005.

Igado, O.O., Glaser, J., Ramos-Tirado, M., Bankoğlu, E.E., Atiba, F.A., Holzgrabe, U., et al., 2018. Isolation of a novel compound (MIMO2) from the methanolic extract of *Moringa oleifera* leaves: protective effects against vanadium-induced cytotoxity. Drug Chem. Toxicol. 41 (3), 249–258. https://doi.org/10.1080/01480545.2017.1366504.

Iqbal, S., Bhanger, M.I., 2006. Effect of season and production location on antioxidant activity of *Moringa oleifera* leaves grown in Pakistan. J. Food Anal. 19, 544–551. https://doi.org/10.1590/sajs.2013/1154.

Jaarsma, D., van den Berg, R., Wulf, P.S., van Erp, S., Keijzer, N., Schlager, M.A., et al., 2014. A role for Bicaudal-D2 in radial cerebellar granule cell migration. Nat. Commun. 5, 3411. https://doi.org/10.1038/ncomms4411.

Kipp, M., Clarner, T., Dang, J., Copray, S., Beyer, C., 2009. The cuprizone animal model: new insights into an old story. Acta Neuropathol. 118, 723–736. https://doi.org/10.1007/s00401-009-0591-3.

Kirisattayakul, W., Wattanathorn, J., Tong-Un, T., Muchimapura, S., Wannanon, P., 2012. *Moringa oleifera* lam mitigates oxidative damage and brain infarct volume in focal cerebral ischemia. Am. J. Appl. Sci. 9 (9), 1457–1463.

Kirisattayakul, W., Wattanathorn, J., Tong-Un, T., Muchimapura, S., Wannanon, P., Jittiwat, J., 2013. Cerebroprotective effect of *Moringa oleifera* against focal ischemic stroke induced by middle cerebral artery occlusion. Oxid. Med. Cell. Longev. 2013, 10.

Lindamood, C., Farnell, D., Giles, H.D., Prejean, J.D., Collins, J.J., Takahashi, K., Maronpot, R.R., 1992. Subchronic toxicity studies of t-Butyl alcohol in rats and mice. Fundam. Appl. Toxicol. 19, 91–100.

Luqman, S., Srivastava, S., Kumar, R., Maurya, A.K., Chanda, C., 2012. Experimental assessment of *Moringa oleifera* leaf and fruit for its antistress, antioxidant, and scavenging potential using in vitro and in vivo assays. Evid. Based Complement. Altern. Med. 2012, 12. https://doi.org/10.1155/2012/519084.

Mohan, M., Kaul, N., Punekar, A., Girnar, R., Junnare, P., Patil, L., 2005. Nootropic activity of *Moringa oleifera* leaves. J. Nat. Remedies 5, 59–62.

Mustapha, O., Oke, B., Offen, N., Sirén, A., Olopade, J., 2014. Neurobehavioral and cytotoxic effects of vanadium during oligodendrocyte maturation: a protective role for erythropoietin. Environ. Toxicol. Pharmacol. 38, 98–111. https://doi.org/10.1016/j.etap.2014.05.001.

Olopade, J.O., Connor, J.R., 2010. Vanadium and neurotoxicity: a review. Curr. Top. Toxicol. 7, 33–39. https://pennstate.pure.elsevier.com/en/publications/vanadium-and-neurotoxicity-a-review.

Olopade, J.O., Fatola, I.O., Olopade, F.E., 2011. Vertical administration of vanadium through lactation induces behavioural and neuromorphological changes: protective role of vitamin e. Niger. J. Physiol. Sci. 26, 055–060. https://www.ajol.info/index.php/njps/article/view/84895.

Olopade, F.E., Shokunbi, M.T., Sirén, A.L., 2012. The relationship between ventricular dilatation, neuropathological and neurobehavioural changes in hydrocephalic rats. Fluids Barriers CNS 9 (19).

Osuji, L.C., Avwiri, G.O., 2005. Flared gases and other pollutants associated with air quality in industrial areas of Nigeria: an overview. Chem. Biodivers. 2, 1277–1289. https://doi.org/10.1002/cbdv.200590099.

Palomba, M., Seke-Etet, P.F., Laperchia, C., Tiberio, L., Xu, Y.-Z., Colavito, V., et al., 2015. Alterations of orexinergic and melanin-concentrating hormone neurons in experimental sleeping sickness. Neuroscience 290, 185–195. https://doi.org/10.1016/J.NEUROSCIENCE.2014.12.066.

Paxinos, G., Franklin, K.B.J., 2001. The Mouse Brain in Stereotaxic Coordinates, 2nd ed. Academic Press, pp. 97–99.

Salonen, J.T., NyyssoèNen, K., Salonen, R., Lakka, H.-M., Kaikkonen, J., Porkkala-Sarataho, E., Voutilainen, S., Lakka, T.A., Rissanen, T., Leskinen, L., Tuomainen, T.-P., Valkonen, V.-P., Ristonmaa, U., Poulsen, H.E., 2000. Antioxidant Supplementation in Atherosclerosis Prevention (ASAP) study: a randomized trial of the effect of vitamins E and C on 3-year progression of carotid atherosclerosis. J. Internal Med 248, 377–386. https://doi.org/10.1046/j.1365-2796.2000.00752.x.

Schmued, L., Bowyer, J., Cozart, M., Heard, D., Binienda, Z., Paule, M., 2008. Introducing Black-Gold II, a highly soluble gold phosphate complex with several unique advantages for the histochemical localization of myelin. Brain Res. https://doi.org/10.1016/j.brainres.2008.06.129.

Singh, R., Rajasree, P.H., Sankar, C., 2012. Suppression of neurofilament degradation by protease inhibitors extracted from *Moringa oleifa* leaves in experimental spinal cord injury. J. Pharm. Res. 5 (10), 4987–4990.

Skripuletz, T., Hackstette, D., Bauer, K., Gudi, V., Pul, R., Voss, E., et al., 2013. Astrocytes regulate myelin clearance through recruitment of microglia during cuprizone-induced demyelination. Brain 136, 147–167. https://doi.org/10.1093/brain/aws262.

Stewart, J.S., Lignell, A., Pettersson, A., Elfving, E., Soni, M.G., 2008. Safety assessment of astaxanthin-rich microalgae biomass: acute and subchronic toxicity studies in rats. Food Chem. Toxicol. 46, 3030–3036.

Sutalangka, C., Wattanathorn, J., Muchimapura, S., Thukham-mee, W., 2013. *Moringa oleifera* mitigates memory impairment and neurodegeneration in animal model of age-related dementia. Oxid. Med. Cell. Longev., 695936. https://doi.org/10.1155/2013/695936.

Tansey, F.A., Cammer, W., 1991. A pi form of Glutathione-S-Transferase is a myelin-and oligodendrocyte-associated enzyme in mouse brain. J. Neurochem. 57, 95–102. https://doi.org/10.1111/j.1471-4159.1991.tb02104.x.

Tripathi, R.B., Rivers, L.E., Young, K.M., Jamen, F., Richardson, W.D., 2010. NG2 glia

generate new oligodendrocytes but few astrocytes in a murine experimental autoimmune encephalomyelitis model of demyelinating disease. J. Neurosci. 30, 16383–16390. https://doi.org/10.1523/JNEUROSCI.3411-10.2010.

Verma, S., Dubey, R.S., 2003. Lead toxicity induces lipid peroxidation and alters the activities of antioxidant enzymes in growing rice plants. Plant Sci. 164, 645–655. https://doi.org/10.1016/S0168-9452(03)00022-0.

World Health Organization (WHO), 2001. Vanadium Pentoxide and Other Inorganic Vanadium Compounds (Concise International Chemical Assessment Document 29), ISBN 92 4 153029 4 (NLM Classification: QV 290). ISSN 1020-6167:1–73. http://www.euro.who.int/_data/assets/pdf_file/0016/123082/AQG2ndEd_6_12vanadium.PDF.

Yuasa, S., Kawamura, K., Ono, K., Yamakuni, T., Takahashi, Y., 1991. Development and migration of Purkinje cells in the mouse cerebellar primordium. Anat. Embryol. (Berl) 184, 195–212. Available at: http://www.ncbi.nlm.nih.gov/pubmed/1724357 [Accessed July 24, 2018].

Zendedel, A., Beyer, C., Kipp, M., 2013. Cuprizone-induced demyelination as a tool to study remyelination and axonal protection. J. Mol. Neurosci. 51, 567–572. https://doi.org/10.1007/s12031-013-0026-4.